AD-

11374

CONFIDENTIAL

009

CONFIDENTIAL
SECURITY INFORMATION

PROJECT MICHAEL

CONTRACT N6-ONR-27135

COLUMBIA UNIVERSITY

HUDSON LABORATORIES

DOBBS FERRY, N. Y.

3744

RESEARCH SPONSORED BY

OFFICE OF NAVAL RESEARCH

CONFIDENTIAL
SECURITY INFORMATION

CU-14-53-ONR-271-Phys

COLUMBIA UNIVERSITY

Hudson Laboratories

Dobbs Ferry, N. Y.

PROJECT MICHAEL

Contract N6-ONR-27135

Technical Report No. 9
30 cps Sound Propagation
in Shallow Water
By
G. E. Becker, R. O. Carlson,
R. A. Frosch, and H. L. Poss

E. T. Booth - Director

J. E. Nafe
Director of Research

Research Sponsored by

Office of Naval Research

CONFIDENTIAL

SECURITY INFORMATION

April 15, 1953

Copy No. 009

Table of Contents

List of Tables

List of Figures

CONFIDENTIAL

30 CPS SOUND PROPAGATION IN SHALLOW WATER

by

G.E.Becker, R.O.Carlson, R.A.Frosch, H.L.Poss

ABSTRACT

The sound field in the neighborhood of a 30 cps frequency stabilized source has been investigated experimentally at two locations in Long Island Sound. In both cases the source was operated at a depth of 40 feet. The two stations have appreciably different water and basement depths. Curves of pressure vs range out to several thousand yards show irregular patterns of maxima and minima with an overall dependance on range which varies from $r^{-1/2}$ to greater than r^{-1}. The minima show no simple azimuthal pattern.

Computations using the normal mode theory have been made for suitable models of the two stations. These computations predict cylindrical symmetry in azimuth and an $r^{-1/2}$ decrease in pressure with range superimposed on a series of maxima and minima. At the station with deeper water and basement depths six propagating modes are predicted. A reasonable choice of parameters for a three layer model yields curves which are similar in appearance to the experimental curves. In one case the spacing of minima agree in some detail. At the shallower station only two propagated modes are expected. A pattern

CONFIDENTIAL
SECURITY INFORMATION

similar to the regular pattern expected from the interference of these modes appears on only one experimental curve.

INTRODUCTION

Earlier experimental investigations of the propagation of low frequency sound in shallow water have been in agreement with the predictions of normal mode theory.[1,2] The practical importance of this subject, for example in the problem of acoustic minesweeping, makes it desirable to extend the range of experimental measurements and compare further the measurements with theory.

During August 1952 a study of shallow water propagation in Long Island Sound was carried out by Hudson Laboratories. Scheduled tests of a powerful frequency stabilized 30 cps source [3] provided the opportunity for mapping the surrounding sound field.

Two different localities in Long Island Sound were chosen for study. Some information on bottom conditions exists for each site. Water and basement depths are nearly constant over a considerable area at each place but the actual thicknesses of water and sediment are such that the number of normal modes propagating differ. With the boundary conditions reasonably simple, it was possible to make a detailed comparison of the experimental results with the predictions of normal mode theory for each site.

SITES

The two locations selected for the shallow water propagation study were chosen after consideration of the charted depths of water in Long Island Sound and the basement contours in the area. Fig. 1 shows the basement contours given by Oliver and Drake[4], and Fig. 2 shows the water depths. The two locations are marked I and II in the figures.

The seismic data of Oliver and Drake gives an average velocity of sound in the rock basement of 18,400 ft/sec or 3.7 times the velocity of sound in water (4950 ft/sec). Above the basement is a layer of clay for which the sound velocity is 5400 ft/sec or 1.1 times the velocity in water. At some positions no difference between the velocities in clay and water was detected. It is possible that the clay has layers of somewhat different densities.

At Station I the water depth is 120 ft. Beneath the water there is the layer of clay and mud about 430 ft deep, and beneath the clay there is a rock basement. The water depth is constant within ± 10% for two miles to the north and west, and for eighteen miles to the east. The clay layer under this flat layer of water increases in thickness at the rather slow rate of fifty feet per mile from north to south. To the north, both the basement depth and the sediment depth decrease. To the south the basement depth increases while the sediment depth decreases.

At Station II, both the water layer and the clay layer increase slowly in thickness from north to south. The water is about 50 to 60 ft deep, over a layer of sediment about 100 ft thick. At their nearest refraction shooting station, Oliver and Drake found no arrival indicating the water sediment interface. The most probable conclusion to be drawn from this fact is that the velocity of sound in the sediment, and its density (at any rate at the interface), is the same as that of the water.

EXPERIMENTAL PART

Apparatus

The sound source for these experiments was an A Mark 6(b) Acoustic Minesweeper, modified as described in a previous report.[3] Details of operation of the 30 cps sound source are covered in reports from this laboratory.[5] The acoustic power output of the source is about 250 watts, from measurements as described in the Appendix. For the operations in Long Island Sound the sound source was suspended from the end of a boom on a self-propelled lighter.

The battery-operated sound receiving equipment was carried on two 40 ft diesel driven workboats, one a Picket boat and the other a Retriever. Each boat was equipped with a boom, a bathythermograph reel, and wire cable. A 30 lb weight on the end of the wire cable caused it to hang nearly vertically. A Brush type AX-58-C hydrophone was tied to the wire just above the weight. The dial reading on the reel then ordinally gave the hydrophone depth directly. The hydrophone cable was kept slack to eliminate one possible source of noise. The signal from the hydrophone was fed into a Woods Hole Model No. 3 Suitcase Amplifier,[6] with an additional LC filter having a Q of nine. (A higher Q would have been advantageous,but suitable equipment was not available when this work was done.)

With this filter, the background reading was of the order of 10 db above one dyne/cm^2, but occasionally went as high as 15 or as low as 5 db above one dyne/cm^2.

The calibration of each amplifier was checked frequently by applying a 30 cps signal of known voltage from an oscillator and a GR Microvolter. The hydrophones were calibrated by placing each in the water near the 30 cps source alongside another hydrophone previously calibrated in combination with a GR type 759-B Sound Level Meter.

Procedure

The experimental work was done during daylight hours in the period August 5 to August 13, 1952 at Station I, and August 14 to August 19, 1952 at Station II. At each station the lighter was anchored and the workboats went out on various azimuths to make their measurements. A workboat carrying a hydrophone was anchored when it was desired to measure the sound intensity as a function of depth at a given position, or when the signal was so little above background that it was necessary to turn the source on and off several times to determine the signal strength. At other times, the workboat was allowed to drift with the current while the depth of the hydrophone was kept constant. The boats drifted with a maximum speed of about one knot in a general easterly or westerly direction. The output meter was watched continuously and readings were made at 15 second intervals in most cases. In order to obtain simultaneous measurements at different depths, some drift runs were made with two hydrophones at different depths. With the particular amplifier available, it was necessary to read the signals from the two hydrophones alternately and it is possible that some fine details of the sound pressure amplitude vs range curves were lost as a consequence. At Station II the currents and wind were weak enough so that it was possible to move a workboat along a desired radial path by pulling it with a line from the lighter. In this way a wider range of azimuth angle was covered than at Station I.

With good visibility the position of the source could be determined by taking sextant bearings on three or more landmarks, with an uncertainty of ± 300 yds on all except one day at Station I, when the visibility was so bad that positions could be determined only by dead-reckoning. The source was brought back on station each day within ± 1000 yds at Station I and within ± 100 yds at Station II, where a marker buoy was used. The lighter was anchored with a single cable, so that it swung around by 180° when the tidal current changed direction. Such a shift changed the sound source position by about 200 ft. However, during the major part of a working day the source position remained fixed with ± 10 ft.

Several methods were used to determine the range from each workboat to the sound source. For ranges from 30 to 1200 yds, distances were found from sextant measurements of the angle subtended by the mast of the lighter, with an estimated uncertainty of ± 5%. For distances from 1200 to 7000 yds, a range finder mounted on the deck of the lighter was used, with an estimated uncertainty of about 2% at the lower and 5% at the upper end of the range. For greater distances, the position of each boat was found from sights on landmarks.

Data, Station I

Drift runs were taken at various azimuths for distances up to 3000 yds at Station I. These runs show a series of minima which continue out to the farthest point reached. The strongest minima were in the region less than 1000 yds distant from the source, with the spacing between minima being irregular and of the order of 70 to 125 yds. In Fig. 3 are plotted the results from two drift runs, taken nearly simultaneously along two parallel paths separated by about 250 ft. The hydrophone depth, 50 ft, was the same for each run. For the solid curve, the output meter was watched continuously, and readings were noted every 15 seconds. For the dotted curve, readings were noted only every 60 sec because the meter was periodically switched to a second channel for another hydrophone at 90 ft depth. Thus the dotted curve might fail to show some fine details. It is seen from the figure that the curves are in fair general agreement. In the range near 700 yds, it is possible that the dotted curve fails to show the big dips for the reason just mentioned.

Fig. 4 shows the simultaneous measurements made from one boat with hydrophones at 50 ft and 90 ft. The variations in intensity are definitely more pronounced at 50 ft. However, a similar run made on another azimuth with hydrophones at 42 ft and 84 ft showed no such behavior, but indicated large variations in intensity at both depths.

The drift runs are listed in Table I. An examination of these data show that, for a given hydrophone depth, many of the minima fall approximately on concentric circles surrounding the sound source, as would be expected for symmetry reasons. However, there are many minima not falling on the circles and, in addition, in many cases expected minima do not appear.

In an attempt to obtain the decay law at large distances, anchored positions (distance stations) were taken at ranges up to eight miles to the east of the source, and four miles to the north. The various positions are listed in the third part of Table I. In Fig. 5 are plotted all the readings made in an easterly direction with the hydrophone at 90 ft. The smooth curve gives the average intensity as a function of distance. Interference maxima and minima, which are too detailed to show on this plot, probably account for the scatter of points about the smooth curve. At distances larger than 4000 yds it was not practicable to take drift runs, since the signal was weak enough that background fluctuations could cause relatively large errors.

Instead, with the work boat anchored, the source was turned on and off several times so that a rather accurate value for the intensity was obtained. Whether this measured point was near a maximum or minimum was not determined, however, and this makes the slope of the curve at large distances somewhat uncertain. The results appear to be incompatible with cylindrical spreading at large distances.

Fig. 6 is a plot of readings made in a northerly direction with hydrophone depths between 75 and 100 ft. In this direction the basement depth steadily decreases, while the water depth remains constant for several miles and then decreases. The high level of sound out to about four miles combined with the sudden drop at that distance suggest that sound may be somehow reflected from the north direction. It should be noted that the two boats did not take exactly the same northerly course, which may account for the difference in observations made from the two boats.

Typical vertical traverse patterns are shown in Fig. 7 and exhibit no new features not observed by Ide.[1] For the more distant positions, curve C is representative. There is a continuous increase in sound level from the surface of the water to the bottom. For the closer positions, curves A, B, and D are representative, the first two having broad minima and the last a sharp minimum at a depth of 50 ft. In other cases sharp minima were observed at depths of 75 ft and 90 ft.

TABLE I

List of Measurements Made at Station I

Vertical Traverses

Date	Boat	Distance in yards	Depth covered in feet	Position of minimum
8/5	Picket	98	10 - 130	Near bottom
		50	10 - 130	60 ft - see Fig. 7A
		160	10 - 125	90 ft - see Fig. 7B
	Retriever	350	10 - 127	75 ft
		36	10 - 124	none
		860	10 - 126	none
		1450	10 - 122	none
8/6	Picket	2030	10 - 110	slight dip at bottom
		4000	10 - 130	none
	Retriever	112	10 - 121	none
		350	10 - 123	75 ft
		200	10 - 111	none
8/7	Picket	3320	10 - 105	slight dip at bottom
		4800	10 - 125	none
		7600	10 - 125	none - see Fig. 7B
		9650	10 - 115	none
8/12	Picket	450	10 - 132	90 ft
8/13	Picket	96	10 - 117	none
		190	20 - 116	none
		268	10 - 119	50 ft - see Fig. 7D

Drift Runs

Date	Boat	Hydrophone depth in feet	Range of run in yards	Remarks
8/7	Retriever	75	725 → 125 → 1500	
8/8	Picket	50	80 → 2950	Many strong minima See Figs. 3 & 23
		75	50 → 1800	Many strong minima
	Retriever	50 & 90	30 → 2350	See Figs. 3 & 4
		30 & 100	25 → 1685	
8/12	Picket	90	350 → 3000	Fewer minima than at 50 & 75 ft
	Retriever	84	500 → 2000	
		84	1100 → 335	
8/13	Retriever	42 & 84	990 → 590 → 1390	

Table I (cont'd.)

List of Measurements Made at Station I

Distance Stations

Date	Boat	Direction	Distance in yards	Hydrophone depth in feet	Sound pressure level db above 1 dyne/cm^2
8/11	Picket	East	2150	90	40.6
			4130	90	18.8
			7700	90	21.3
			12800	90	19.5
			15600	90	13.5
			4000	90	35.4
	Retriever	North	1850	100	41.4
			3950	99	38.9
			8000	86	15 near background
			6000	99	38.5
			7600	91	33.1
8/13	Picket	North	7500	75	15.3 (background ~5)
			6900	75	22.0

Data, Station II

All the runs at this station are listed in Table II. Because of the more rapid decrease of sound intensity with distance at this station (as compared with Station I), a more complete survey could be made in the time available to us, covering a larger range of azimuth angle. Because the currents and winds were relatively weak it was possible to move a workboat along an arbitrary radial path by pulling it with a line from the lighter.

Data from five of these "pull-in" runs and two drift runs are plotted in Figs. 8, 9, 10, 11, and 12. In these runs the hydrophone depth was 30 ft, except Fig. 12, where it was 25 ft. It is apparent that the spacing of the minima is not at all regular. Furthermore, there is little evidence that the minima occur at the same radial distances for all azimuths. The chief exception to this is the minimum near 580 yds, which appears on almost all of the curves. Another feature seen from these curves is that the average sound level decays at about the same rate with distance in all directions. A comparison with the curves for Station I shows that the rate of attenuation is definitely greater in the shallower water at Station II.

Fig. 13 is a plot of sound pressure as a function of depth (vertical traverse) at several ranges.

TABLE II

List of Measurements Made at Station II

Vertical Traverses

Date	Boat	Distance-yards	Depth-feet	Remarks
8/14	Retriever	500	3 - 47	No minimum
	Picket	13	3 - 49	No minimum
8/15	Retriever	60	3 - 45	Definite minimum at 35 ft
		56	3 - 45	No minimum

Drift Runs

Date	Boat	Run	Hydrophone depth in feet	Range of run in yards	
8/14	Retriever	I	25	625 → 480 → 487	
		II	25	100 → 475	
8/15	Retriever	I	25	38 → 860	See Fig. 12
	Picket	I	30	322 → 107	
		II	30	515 → 1280	See Fig. 11
8/18	Retriever	I	25	310 → 1780	
		II	25	1066 → 190 → 1500	
	Picket	I	40	700 → 230	
		II	30	590 → 55	See Fig. 10
		III	30	630 → 130	See Fig. 9
		IV	30	625 → 90	See Fig. 9
		V	30	700 → 90	
		VI	30	850 → 270 → 1060	
8/19	Retriever	I	40	590 → 1540	
	Picket	I	30	1600 → 80	See Fig. 8
		II	30	1515 → 180	See Fig. 10

Distance Stations

Date	Boat	Direction	Distance in yards	Hydrophone depth in feet	Sound pressure level db above 1 dyne/cm²	
8/14	Picket	South	2000	50	15.3	
			3100	50	13.3	
			4600	50	6.3	
8/15	Picket	East	860	30	42.7	No minima were
			1210	30	42.6	found in ver-
			1570	30	28.4	tical traverses
			1945	30	25.0	at any of these
			2010	30	19.0	East stations

THEORETICAL PART

Normal Mode Theory

The theory of the propagation of sound in a medium composed of parallel sided slabs has been developed by Pekeris[2] and by Ide, Post, and Fry.[1] The development by Pekeris is somewhat more extended and rigorous and for these reasons we shall refer mostly to his work, using his notation. Pekeris develops the theories of two systems, using the same approach in both cases.

The first system consists of a parallel sided slab of a medium I with density ρ_1, and sound velocity c_1. The top face at $z = o$ is bounded by a free (pressure = 0) surface, and the bottom face at $z = H$ is bounded by medium II with density ρ_2 and sound velocity c_2. This second medium extends downwards indefinitely.

The second system is identical with the first except that the second slab is of thickness h, and is bounded at its bottom face $(z = H + h)$ by medium III with density ρ_3 and sound velocity c_3.

We shall refer to the first system as the two layer case, and to the second system as the three layer case. In each case the top layer will be water, and the bottommost layer, referred to as the basement, will be rock. In the three layer case the intermediate layer will be mud, clay, or sediment of some sort.

It will be assumed that the only waves propagating in these media are compressional. Any shear waves which might be propagated in the basement or in the sediment are neglected.

If z is the vertical coordinate and r the horizontal radial coordinate of a cylindrical coordinate system in both the two and three layer cases, Pekeris finds the pressure of the sound field everywhere due to a unit point source at $r = 0$ and $z = d$, where $d < H$. The solution is first exhibited as two (or three) integrals, each over an auxiliary complex variable k. Each integral provides the solution in one of the media of the system. The integrands are such that the integrals satisfy the appropriate wave equations and the boundary conditions.

The integrals are then each evaluated as an integral along a branch line in the k plane, plus the sum of the residues at the (infinitely many) poles of the integrand in the k plane. It is shown that under certain conditions (which are satisfied in our case) the branch line integral behaves as r^{-2} (for the pressure) for large r, and thus appears to correspond to the reactive field near the source. We have neglected this branch line integral in our computations, and considered only the series of residues, referred to as the "Normal Modes."

In both the two and three layer cases the normal mode series for the pressure in this region $0 < z < H$ may be written as

$$(1)\quad \phi = \frac{2\pi}{H}\sqrt{\frac{2}{\pi r}}\sum_{n=1}^{\infty}\frac{1}{\sqrt{k_n}}\,e^{i(\omega t - k_n r - \frac{\pi}{4})}\,F(x_n)\sin\left(\frac{x_n d}{H}\right)\sin\left(\frac{x_n z}{H}\right)$$

In this series the large r approximation,

$$(2)\quad H_o^2(k_n r) \rightarrow \sqrt{\frac{2}{\pi k_n r}}\;e^{i(\frac{\pi}{4} - k_n r)}$$

has been made, where H_0^2 is the Hankel function of zero order of the second kind (corresponding to outgoing waves with the time dependance $e^{i\omega t}$). This approximation is generally satisfactory for $r > \lambda$ and improves with increasing r. The difference between the two and three layer cases appears in the function $F(x_n)$ which is different in the two cases. It should be noted that the $r^{-1/2}$ provides overall cylindrical spreading in all cases, while the quantities sin $\left(\frac{x_n d}{H}\right)$ and sin $\left(\frac{x_n z}{H}\right)$ make the pressure everywhere zero for source or receiver at the surface. The quantity $k_n = \sqrt{\frac{\omega^2}{c_1^2} - \frac{x_n^2}{H^2}} = \frac{\omega}{c_n}$, where c_n is the phase velocity of the n^{th} mode. The values of k_n are the positions of the poles of the integrand in the original integral solution for the pressure, and are obtained by solving a transcendental equation arising from the specification of these poles. Given the k_n, the c_n and x_n may be found as above. The transcendental equations for the two and three layer cases differ.

The normal mode solution is particularly convenient in the cases $c_1 < c_2$ and $c_1 < c_2 < c_3$ which correspond to the situations of interest to us. In these cases the k_n and x_n for n less than some n_0 are real while the k_n and x_n for $n > n_0$ are complex and the k_n have negative imaginary parts. Thus the modes for $n < n_0$ propagate undamped, while the modes with $n > n_0$ contain the factor $e^{-\delta r}$ (where δ is the absolute value of the imaginary part of k_n) and hence damp out with increasing r. In general these damping constants increase with increasing $n > n_0$. We have computed the damping constant of the lowest damped mode in one of our cases. The damping was sufficiently fast that the mode had negligible amplitude at any distance from the source where measurements were made. Consequently, in all our computations we have considered only the undamped modes, those with real k_n. When x_n is real it lies in the range $\pi(n-\frac{1}{2}) < x_n < n\pi$ for the n^{th} mode. c_n is thus more than c_1 for the lowest mode and approaches c_2, or c_3 for the three layer case, as the number of the propagated mode increases.

It may be shown that each normal mode corresponds to the sum of a pair of plane waves with equal angles with the horizontal traveling obliquely upward and downward, respectively. The propagated modes correspond to plane waves whose angle of reflection at the bottom is greater than the critical angle, so that they are totally reflected, while the damped modes correspond to plane waves whose angle of reflection at the bottom is less than the critical angle, so that they are partly reflected and partly refracted into the lower medium. The damping of the unpropagated modes thus corresponds to refraction of a portion of the wave into the lower medium as it travels in the r direction.

In our computations we have considered only the propagated modes.

Calculations for Station I

Computations of the sound pressure as a function of r were made using the three layer normal mode theory with various values of sediment density ρ_c , basement density ρ_r, detector depths z, and two values for the width of the sediment layer. In all cases the source depth d was taken to be 40 ft, the water density ρ_w = 1.0, and the velocities of sound in water, sediment, and rock as 4950 ft/sec, 5550 ft/sec, and 18,000 ft/sec, respectively. The water depth (to the top of the sediment layer) was 120 ft. In all cases it was found that six modes were propagated with the approximate phase velocities in ft/sec (for the case h = 430 ft, $\frac{\rho_c}{\rho_w} = 1.5$, $\frac{\rho_r}{\rho_w} = 2.5$):

$$c_1 = 5434 \qquad c_4 = 6782$$
$$c_2 = 5691 \qquad c_5 = 8544$$
$$c_3 = 6061 \qquad c_6 = 14508$$

Higher modes have complex phase velocities and damp out rapidly with range. Since the phase velocity of the first mode is less than the free medium sound velocity in the sediment this mode may be considered to be propagated in the layer of water. The higher modes propagate in the region between the top surface of the water and the basement surface. This is meant in the following senses: If the boundary between the sediment and the basement were extended to minus infinity, so that the three layer case goes over to the two layer case, then the first mode would be propagated while the higher modes would be damped. In the three layer system the plane waves corresponding to the first mode are reflected from the water-sediment interface at an angle greater than the critical angle, and thus are totally reflected. The plane waves corresponding to the higher propagated modes are reflected from the water-sediment interface at angles less than the critical angle, and from the sediment-basement interface at angles greater than the critical angle. The first mode thus travels in the water layer, while the higher propagated modes ($n = 2$ to 6) travel partly in the water layer and partly in the sediment layer.

The various three layer normal mode computations are plotted in Figs. 14, 15, 16. The formula from which these graphs were plotted is too complicated to permit simple conclusions (other than the overall cylindrical spreading factor $r^{-1/2}$) to be drawn directly from the formula.

Examination of Fig. 14 shows that the effect of varying the densities is principally to change the depths of the minima without shifting their positions. Tow of the minima (at 700 and 2220 ft) are decreased in amplitude sufficiently as to virtually disappear. Somewhat wider variation of density would lead to patterns containing fewer minima. The basement density is probably between 2.4 and 2.9 g/cm^3 and the sediment density between 1.1 and 2.0 g/cm^3.

Fig. 14 also shows the change in pattern arising from an increase of 11% in h, the thickness of the sediment layer. The effect of the increase is to spread out the patterns of minima, deepening some of the minima somewhat. With h = 430 ft, minima appear at r = 200, 425, 730, 1030, 1300, 1600, 1880, 2220, and 2430 ft, whereas with h = 480 ft (and the same densities as before) the same minima (judging from their shape) appear at 250, 560, 920, 1400, 1600, 2100, and 2500 ft. It should be noted that the computed patterns for r less than several hundred feet are probably somewhat incorrect because of the approximation made in taking only the propagated normal modes.

Figs. 15 and 16 show the effect on the radial pattern of varying the receiver depth, for two different thicknesses of sediment. It is clear that the deeper the receiver(at any rate below 50 ft) the less pronounced the minima. The effect is particularly pronounced for the 90 ft receiver depth with the 480 ft sediment thickness, where no sharp minima at all appear out to a 2000 ft range, whereas the plot for the 50 ft receiver depth shows seven pronounced minima in this range. Five of these minima are quite sharp and deep.

Sound pressure as a function of depth z for various values of range r is shown in Figs. 17 and 18. Note the extreme change in curve shape between $r = 9750$ ft and $r = 10{,}000$ ft.

Calculations for Station II

Since the sediment layer near Station II has apparently very similar velocity and density values to that of water, the sediment layer can be lumped with the water and the system treated as a two layer case. Only two modes are propagated in this region, consequently the formula for the sound pressure is fairly simple. In arbitrary units, we have, for a basement depth of 160 ft, source depth 40 ft, and assumed basement density and velocity of 2.5 g/cm^3 and 19,000 ft/sec, respectively:

$$(3)\quad \frac{\left[\sin^2(.0145z)+5.429\sin^2(.0308z)+4.66\sin(.0145z)\sin(.0308z)\cos(.0398r)\right]^{1/2}}{r^{1/2}}$$

In this formula z is in feet and r in yards. Aside from the cylindrical spreading factor ($r^{-1/2}$), this is a periodic function of r. It has minima at the points

$$(4)\qquad 0.0398\, r = (2n + 1)\pi$$

Successive minima are thus separated by 158 yds. The vertical pattern is the same for all values of r corresponding to the same point of the cycle, e.g., all minima. The appearance of the function for $z = 30$ ft may be seen from Fig. 19 while in Fig. 20 curves are drawn showing the vertical patterns at a maximum, a minimum, and between a maximum and minimum of the cycle. From the formula it is apparent that the amplitude of the minima increases with increasing depth to 60 ft, the water sediment interface.

A three layer computation has been made for $H = 60$ ft, $h = 100$ ft, $\rho_c/\rho_w = 1.5$, $\rho_r/\rho_w = 2.5$, and $c_1 = 4950$, $c_2 = 5400$, $c_3 = 18{,}400$ ft/sec. The form of the resulting expression for sound pressure vs range and depth is the same as eqn. (3), with different constants. The predicted minimum depth is about 3 db and the spacing between minima is 170 yds. Fig. 21 is a plot of the vertical pattern to be expected at a maximum, a minimum, and between a maximum and a minimum. The sound amplitude reference level is not the same as for Fig. 20. The two figures are very similar in appearance.

The spacing of minima in a sound level vs range curve and the depth of the minima were calculated, using the two layer theory, as a function of two parameters. These parameters were the ratio of basement density to water density or ρ_r/ρ_w and the basement depth H. The following table summarizes the results of the computation.

TABLE III - STATION II

Spacing and Depth of Minima as
Calculated from Two Layer Normal Mode Theory

	H = 140 feet		H = 160 feet	
	Minima		Minima	
	Depth db	Spacing yds	Depth db	Spacing yds
2.0	4.31	109	4.31	155
2.2	4.10	109	4.08	155
2.4	4.62	112	3.87	156
2.6	3.96	112	3.84	155
2.8	3.79	112	3.64	156

	H = 180 feet		H = 200 feet	
	Minima		Minima	
	Depth db	Spacing yds	Depth db	Spacing yds
2.0	4.35	205	4.35	258
2.2	4.15	205	4.15	258
2.4	3.91	203	3.96	258
2.6	3.86	203	3.91	262
2.8	3.76	205	3.78	262

THEORY vs EXPERIMENT

Station I

Let us now compare the theoretical plot of Fig. 22 (similar to one of the curves in Figs. 14 and 15) with the experimental curve of Fig. 23 (same Picket run as in Fig. 3 in greater detail). Both curves are drawn to the same scale, the factor of 100 in the log plot of Fig. 22 corresponding to 40 db in pressure, the range of Fig. 23. The two plots are quite similar in overall appearance, particularly at ranges less than 4900 ft. The experimental curve has an overall fall off with range which is clearly greater than the $r^{-1/2}$ of the theoretical curve.

It is possible to correlate some of the minima on the two curves, especially for ranges below 3900 ft. A listing of similar minima is given below, the numbers representing the approximate range position:

Theoretical Curve Figure 22	Experimental Curve Figure 23
900 feet	900 feet
1400	1300
1650	1500
2100	2000
2500	2300
2700	2700 (double minima)
3200	3200
3600	3400
3900	3800

The preceding correlation is made from the appearance of the two patterns. Correlated minima often do not agree well as to intensity even over the restricted range discussed.

Fig. 4 shows a case in which there is much less minimum structure for the detector at 90 ft as compared to that at 50 ft. This effect is seen in the theory (Figs. 15 and 16). As previously remarked, this effect is not present in all runs.

Let us now turn to a comparison of the theoretical and experimental vertical patterns, i.e., sound pressure as a function of z for a given r. The experimental curve taken at 50 yds = 150 ft bears some resemblance to the theoretical curve (Figs. 17 and 18) for 150 ft (taking account of the difference in scale), but close examination shows the resemblance to be rather superficial. The experimental curves for 160 yds and 7600 yds appear to find no counterparts among the theoretical curves, unless the former corresponds to the curve for $r = 1000$ ft, which seems unlikely. The experimental curve for 268 yds is rather similar in appearance to the theoretical plot for 550 yds. None of the experimental vertical traverses is well matched by a theoretical curve.

The data from Station I appear to have the type of variation found in the computed curves, but do not agree with the theory in detail. In particular, the overall drop in pressure with distance is incorrectly predicted, as may be seen from Figs. 3, 3A & 3B, 4, 4A & 4B, 5-5A & 5B.

The theory predicts that the pressure will vary with range r as $r^{-1/2}$. If the logarithm of this factor, multiplied by 20 to convert to decibels, be subtracted from the original data, then the corrected curve (A) should oscillate about a straight line. ("Corrected" data = original data - 20 log $r^{-1/2}$ = original data + 10 log r). On the other hand, if the radial dependance is other than $r^{-1/2}$, the data corrected for cylindrical spreading should show a slope different from zero. (For an r^{-1} or spherical factor, "corrected" data = original data - 20 log r^{-1} = original data + 20 log r).

The experimental data in the figures referred to do not give quite a straight line when corrected for cylindrical spreading; on the other hand, correction for a spherical spreading or r^{-1} factor causes a rising line. The conclusion from the data is that the spreading loss of signal amplitude is somewhat greater than cylindrical spreading and definitely less than spherical spreading.

Station II

Of the experimental curves taken, only that shown in Fig. 12 bears any resemblance to the theory. The successive spacings between minima in Fig. 12 are 95, 150, and 120 yds. The first experimental minimum occurs at 70 yds. The theory would place it at about 80 yds. However, the theoretical curve is based on z = 30 ft while Fig. 12 data were taken at 25 ft.

On the other curves the minima spacings are irregular and vary from 40 to 140 yds. The curves shown are representative of the data. The minimum at 580 yds is the only one that appears on almost every drift or pull-in run, but most runs had additional minima at one or more of the following ranges: 150, 260, 390, 700, and 810 yds.

In Table III, it was shown that for a change in basement depth H from 200 ft to 140 ft, for reasonable values of rock basement densities, the theoretical minima spacing would change from about 260 yds to 110 yds, which agrees only partially with the experimental minima spacing values. As to minima depth, theory predicts only values of the order of three to five decibels while experimental minima are larger than twenty decibels in some cases, with many minima of the order of ten decibels.

Figs. 20 and 21 show the expected variation of intensity with depth at three positions in the range cycles for the two models. The experimental curves are shown in Fig. 13. It is apparent that only one of the experimental curves disagrees with the theoretical curves, that for 60 yds from the source. It is possible that this deep minima may arise from the effect of the neglected damped modes which are present close to the sound source.

DISCUSSION

It is apparent from the theory vs experiment sections that the normal mode theory can provide an explanation for parts of the overall picture of the sound field surrounding a low frequency shallow water source. The presence of maxima and minima, for example, is very simply explained as arising from the interference of normal modes. At each Station, there is some experimental data which can be approximately fitted by the theory with a suitable, and reasonable, choice of parameters.

However, the fact that at neither experimental Station is the sound field cylindrically symmetric about the source indicates that the boundary conditions are not at all simple. Indeed, very little is known of the sediment layer properties; this layer may be inhomogeneous, containing boulders, gravel, etc., which give back confused reflections to destroy the interference patterns expected in normal mode theory. There may be a layer in the sediment with a velocity lower than the surrounding layers or than the water. Such a layer would tend to trap sound into travelling in it as a duct, providing a continuous loss of sound from the water into the sediment not accounted for by the $r^{-1/2}$ spreading loss of theory. In addition, the sediment may have a real volume absorption for sound of 30 cps frequency to provide a further sound loss.

In view of this lack of knowledge of the boundary conditions at each site in Long Island Sound, it is not surprising that the normal mode theory is inadequate to predict the finer details of the experimental data, such as the minima spacing and depths. Before a real test of the theory can be made with experimental data, it will be necessary to have a more complete knowledge of the specific properties of the sound propagating media.

. . . .

We wish to acknowledge the valuable contributions of Mr. G. T. Aldrich, Dr. M.V. Brown and Mr. L. P. Goldberg in the experimental work.

APPENDIX

Source Output

The sound output of the source was determined by suspending calibrated hydrophones over the side of the lighter, close to the source. Results are listed in Table IV. With the assumption that the pressure obeys a (1/r) law near the source, the measurements may be referred to the standard distance of 6 ft. The values thus found fall in the range 158 - 165 db above .0002 dynes/cm^2, in reasonable agreement with the value of 164 db quoted by the Navy Bureau of Ships. The corresponding power output is approximately 250 watts. The variations in the observed values may possibly be produced by the effects of hull vibrations of the lighter.

The power output of the source was monitored for an hour or more on several occasions, and no significant changes were observed.

TABLE IV

Absolute Sound Levels Measured with Hydrophones over the Side of the Lighter at a Depth of Forty Feet

Date	Detector	Hydrophone Depth	Distance Source to Hydrophone	Measured Signal Strength	Extrapolated Signal Strength
14 Aug 1952	A	24'	25.6'	152	164.6
6 Aug 1952	B	40'	38'	143	159
6 Aug 1952	B	100'	71'	137	158.5
6 Aug 1952	B	50'	77'	139	161
12 Aug 1952	B	40'	17.8'	150	159.5
12 Aug 1952	B	40'	14'	151	158.3

Detector A - Brush AX-58-C Hydrophone and General Radio Sound Level Meter.

Detector B - Massa Hydrophone and Hewlitt-Packard Voltmeter.

Measured Signal Strength in decibels above 0.0002 dynes/cm^2.

Extrapolated Signal Strength at range r = 6' assuming an r^{-1} pressure law in decibels above 0.0002 dynes/cm^2.

REFERENCES

1. J. M. Ide, R. F. Post, W. J. Fry, Naval Research Laboratory. NRL report no. S-2113, The propagation of underwater sound at low frequencies as a function of the acoustic properties of the bottom. August 15, 1943.

2. The Geological Society of America, Memoir 27. Propagation of sound in the ocean. (Papers by M. Ewing, J. L. Worzel, C. L. Pekeris.) October 15, 1948.

3. H. C. Beck, H. Sonnemann, Columbia University, Hudson Laboratories. Technical report no. 8, Conversion of the A Mark 6 (b) minesweeping gear to a 30 cycle sound source. February 10, 1953.

4. J. E. Oliver, C. L. Drake. Geophysical investigations of the emerged and submerged Atlantic coastal plain. Part 6, the Long Island Sound area. Geol. Soc. Am., Bull. vol. 62, p. 1287-1296. (1951).

5. Columbia University, Hudson Laboratories. Quarterly progress report, July 1, 1952. Quarterly progress report, October 1, 1952.

6. W. Dow, Woods Hole Oceanographic Institution. Reference no. 52-10, An experimental portable listening device for detection, measurement and recording of underwater sound. March 1952.

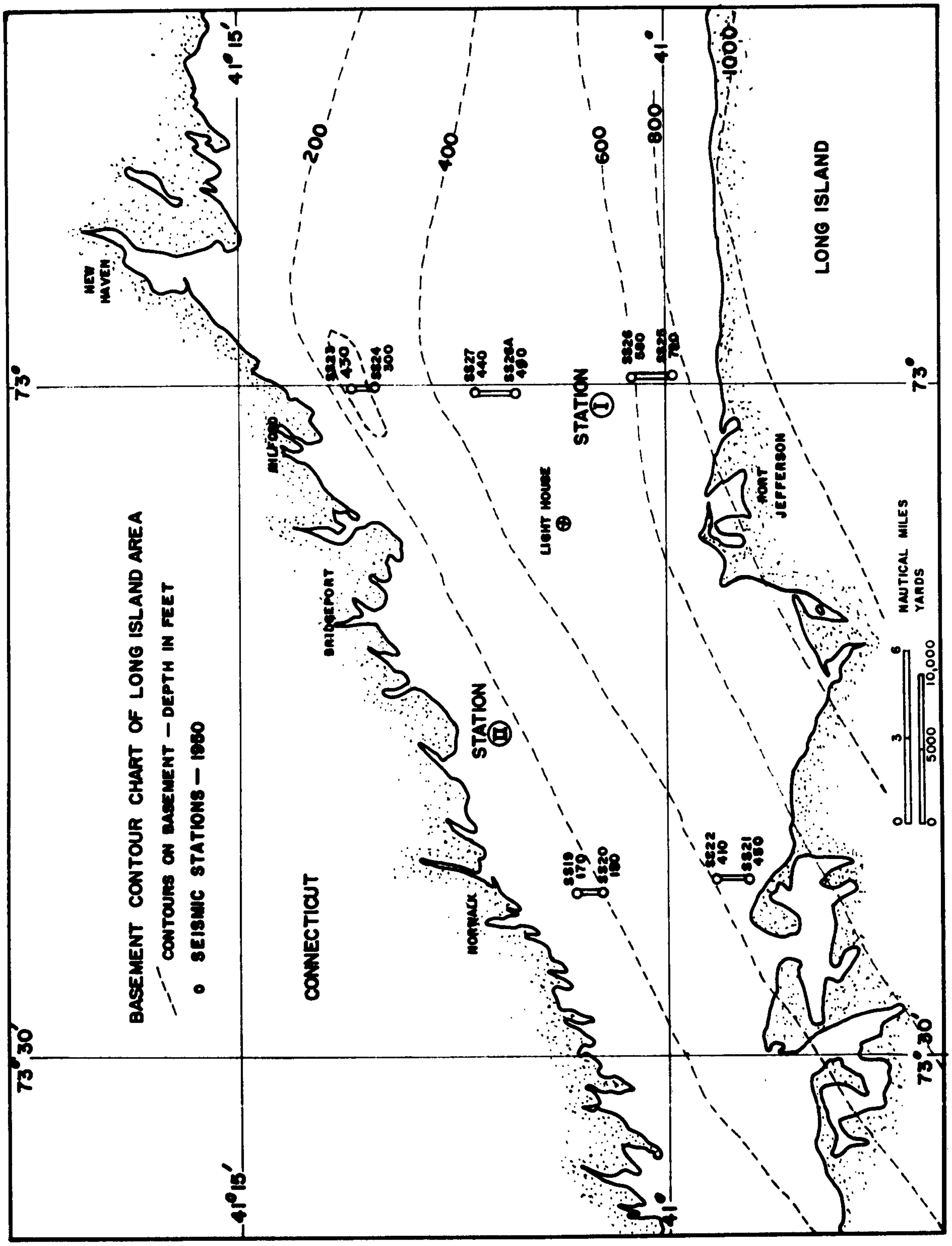
BASEMENT CONTOUR CHART OF LONG ISLAND AREA
CONTOURS ON BASEMENT — DEPTH IN FEET
SEISMIC STATIONS — 1950
CONNECTICUT
LONG ISLAND
NEW HAVEN
MILFORD
BRIDGEPORT
NORWALK
PORT JEFFERSON
LIGHT HOUSE
STATION I
STATION II
200
400
600
800
1000
SS19 170
SS20 180
SS21 450
SS22 410
SS23 430
SS24 300
SS27 440
SS26A 490
SS26 580
SS25 760
NAUTICAL MILES
YARDS
0 3 6
0 5000 10,000
41° 15'
41°
73°
73° 30'

Figure 1

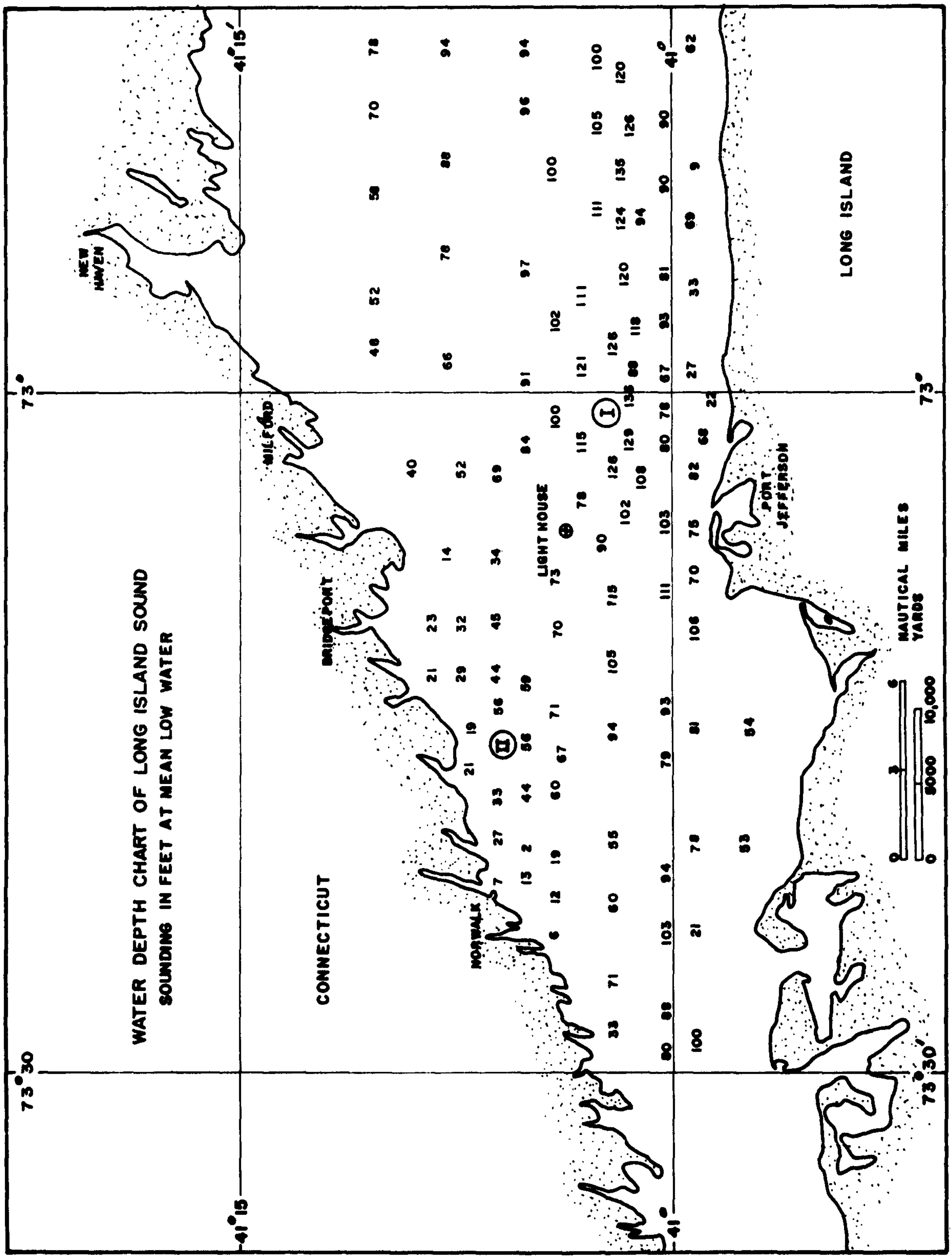
WATER DEPTH CHART OF LONG ISLAND SOUND
SOUNDING IN FEET AT MEAN LOW WATER
CONNECTICUT
LONG ISLAND
NEW HAVEN
MILFORD
BRIDGEPORT
NORWALK
PORT JEFFERSON
LIGHT HOUSE
NAUTICAL MILES
YARDS

Figure 2

CONFIDENTIAL
SECURITY INFORMATION

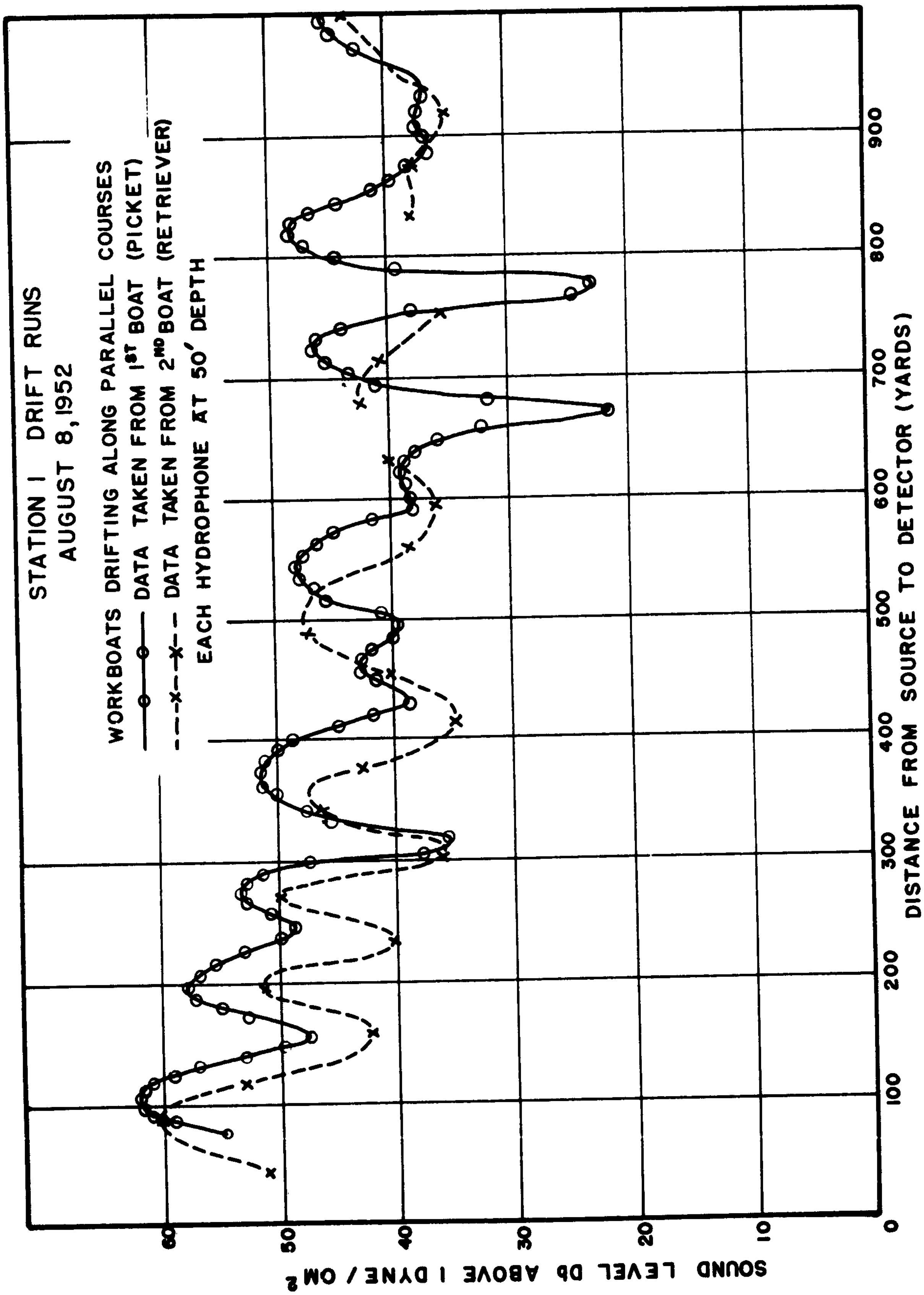

Figure 3

CONFIDENTIAL
SECURITY INFORMATION

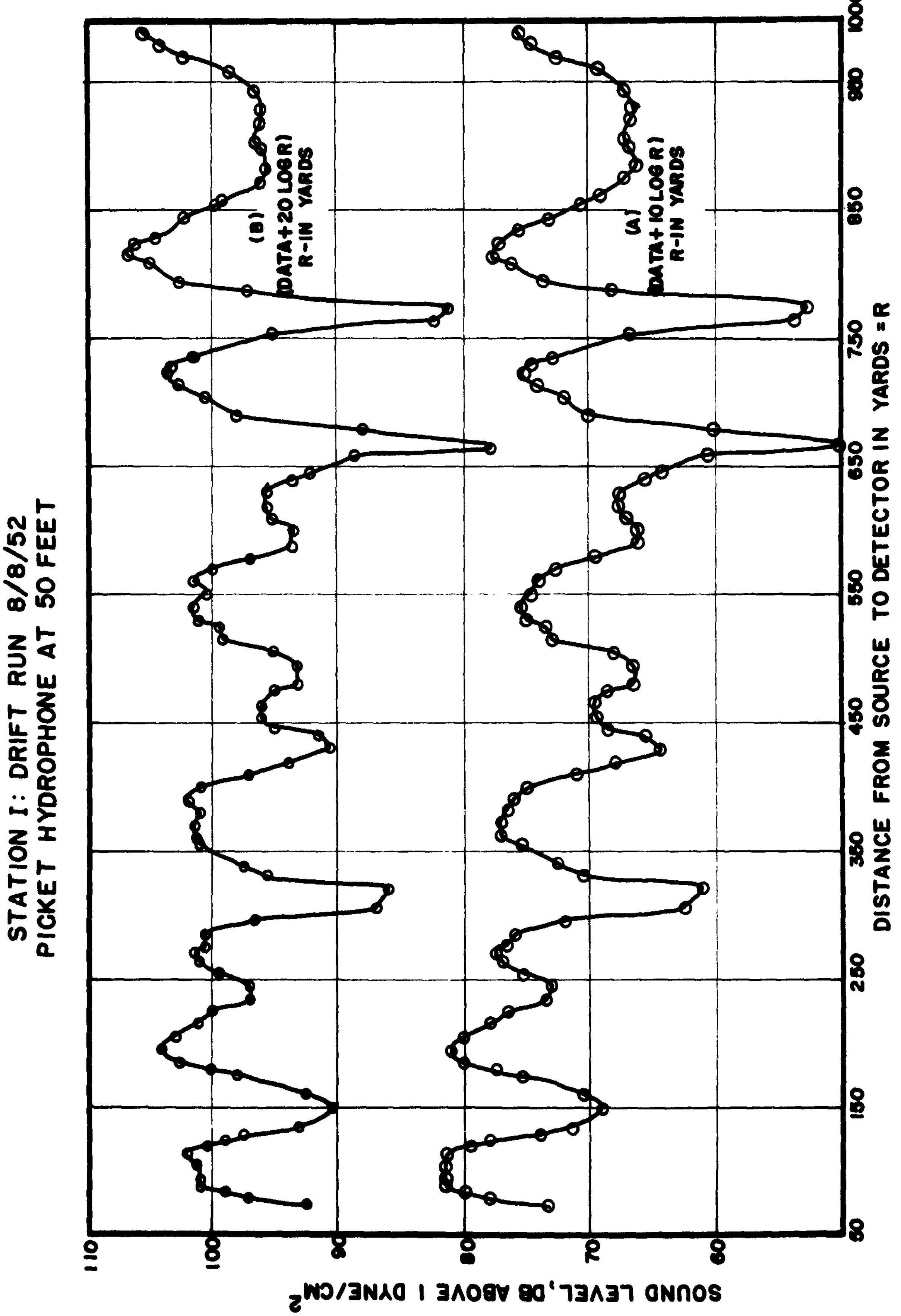
STATION I: DRIFT RUN 8/8/52
PICKET HYDROPHONE AT 50 FEET
(B) DATA+20 LOG R) R-IN YARDS
(A) DATA+10 LOG R) R-IN YARDS
DISTANCE FROM SOURCE TO DETECTOR IN YARDS = R
SOUND LEVEL, DB ABOVE 1 DYNE/CM²
50
150
250
350
450
550
650
750
850
950
1000
110
100
90
80
70
60

Figure 3A & 3B

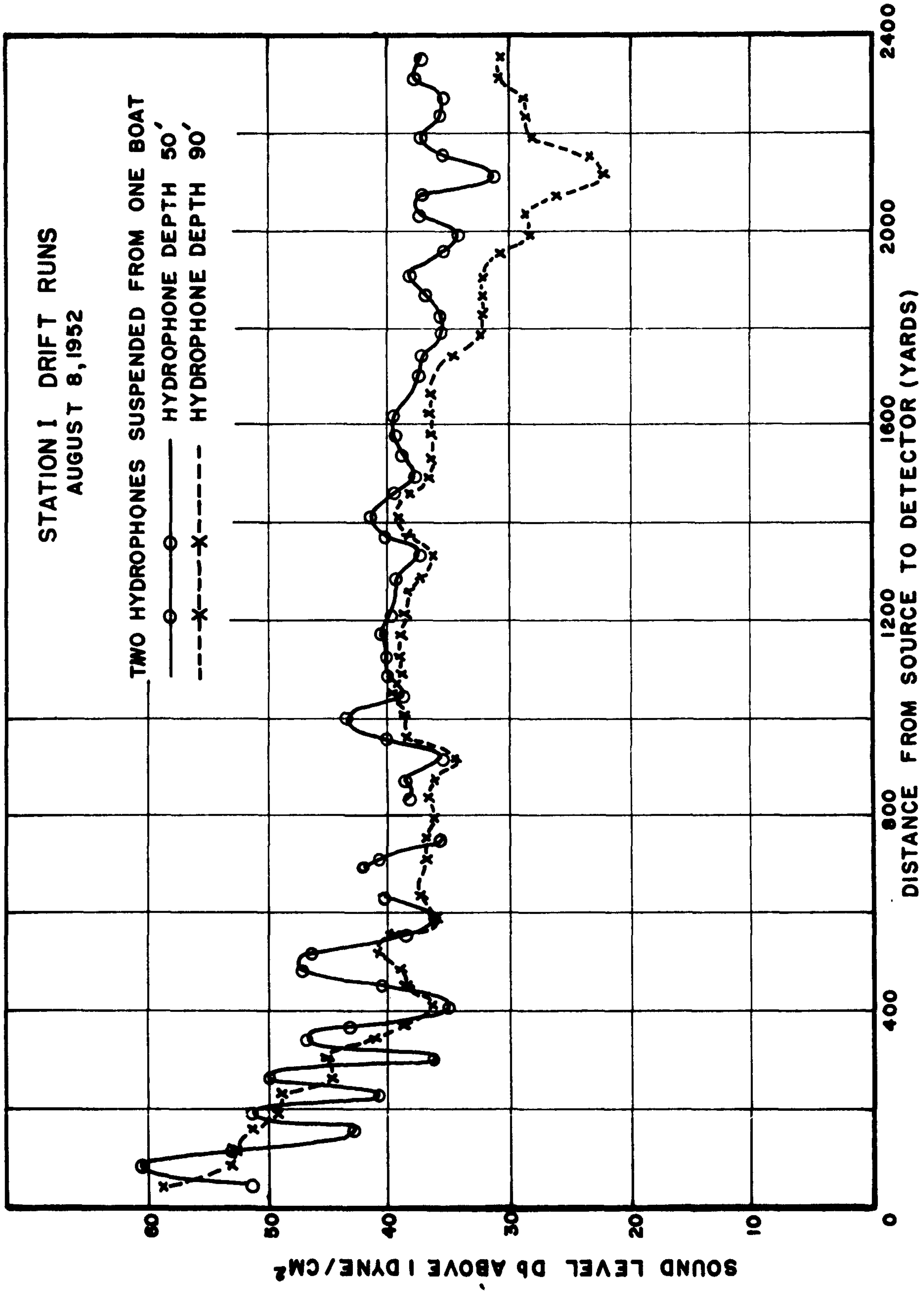
STATION I DRIFT RUNS
AUGUST 8,1952
TWO HYDROPHONES SUSPENDED FROM ONE BOAT
HYDROPHONE DEPTH 50'
HYDROPHONE DEPTH 90'
0
400
800
1200
1600
2000
2400
DISTANCE FROM SOURCE TO DETECTOR (YARDS)
60
50
40
30
20
10
SOUND LEVEL Db ABOVE I DYNE/CM²

Figure 4

CONFIDENTIAL
SECURITY INFORMATION

STATION I : DRIFT RUN 8-8-52
RETRIEVER HYDROPHONE AT 50 FEET

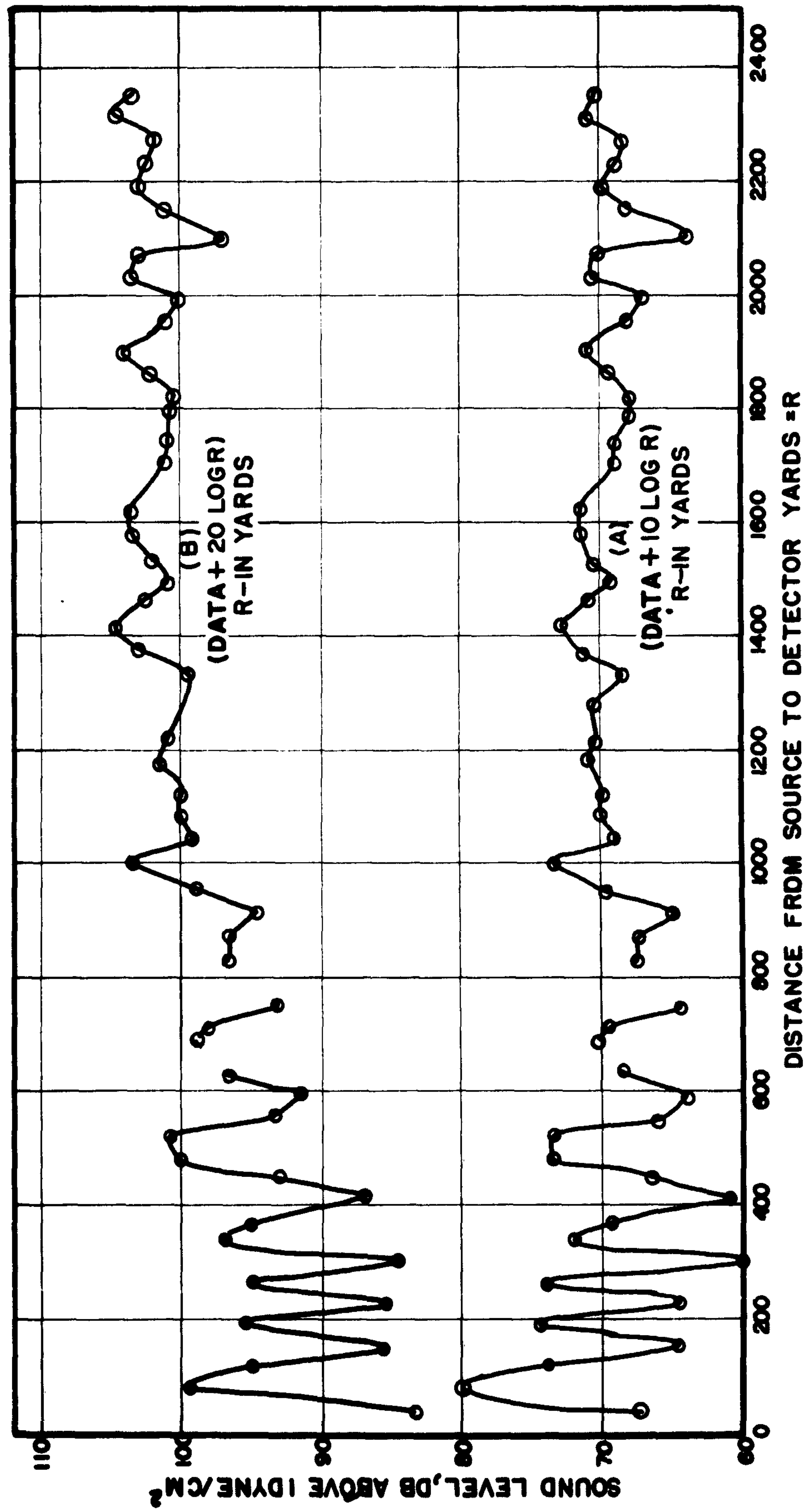

Figure 4A & 4B

CONFIDENTIAL
SECURITY INFORMATION

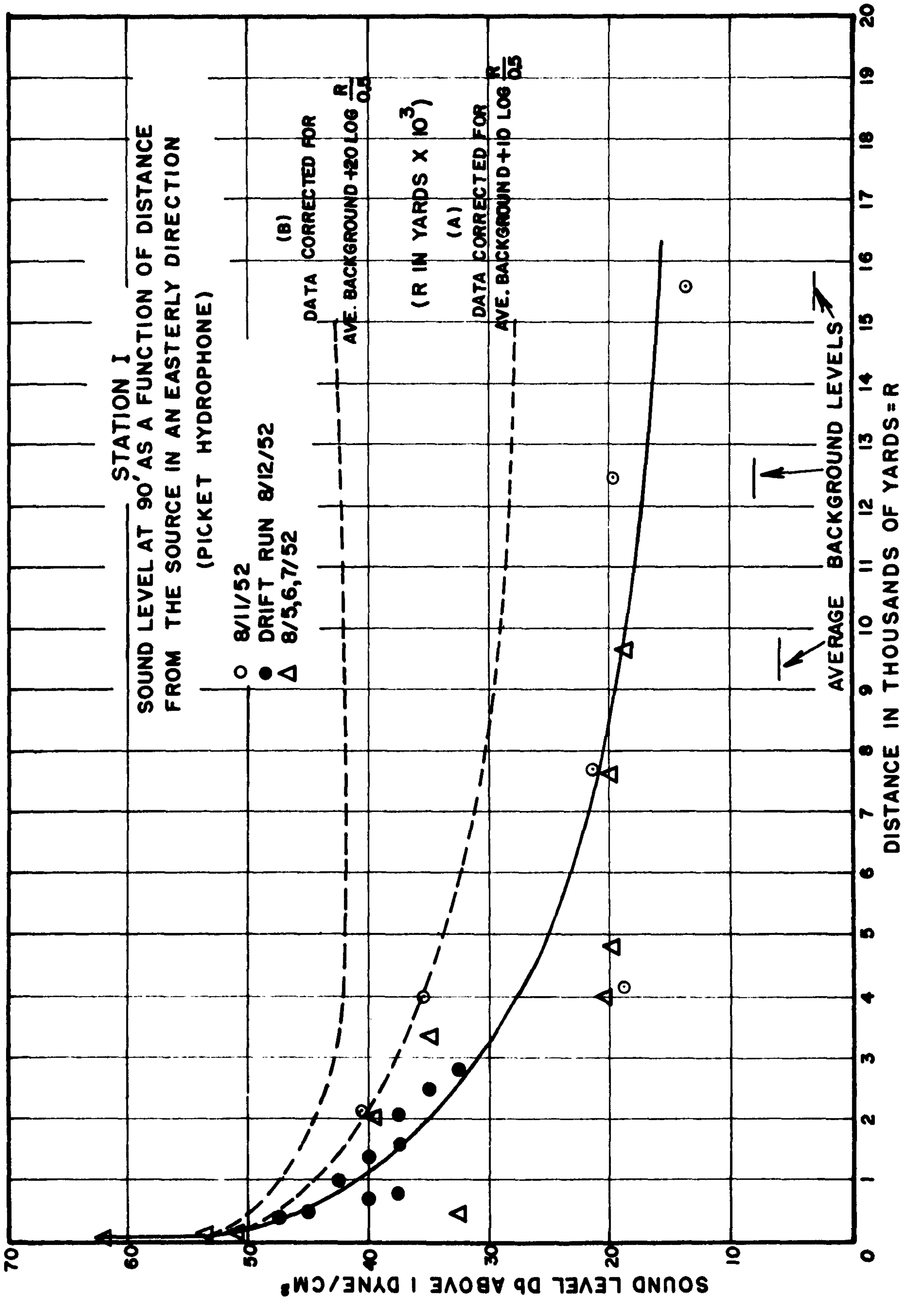

Figure 5 - 5A & 5B

CONFIDENTIAL
SECURITY INFORMATION

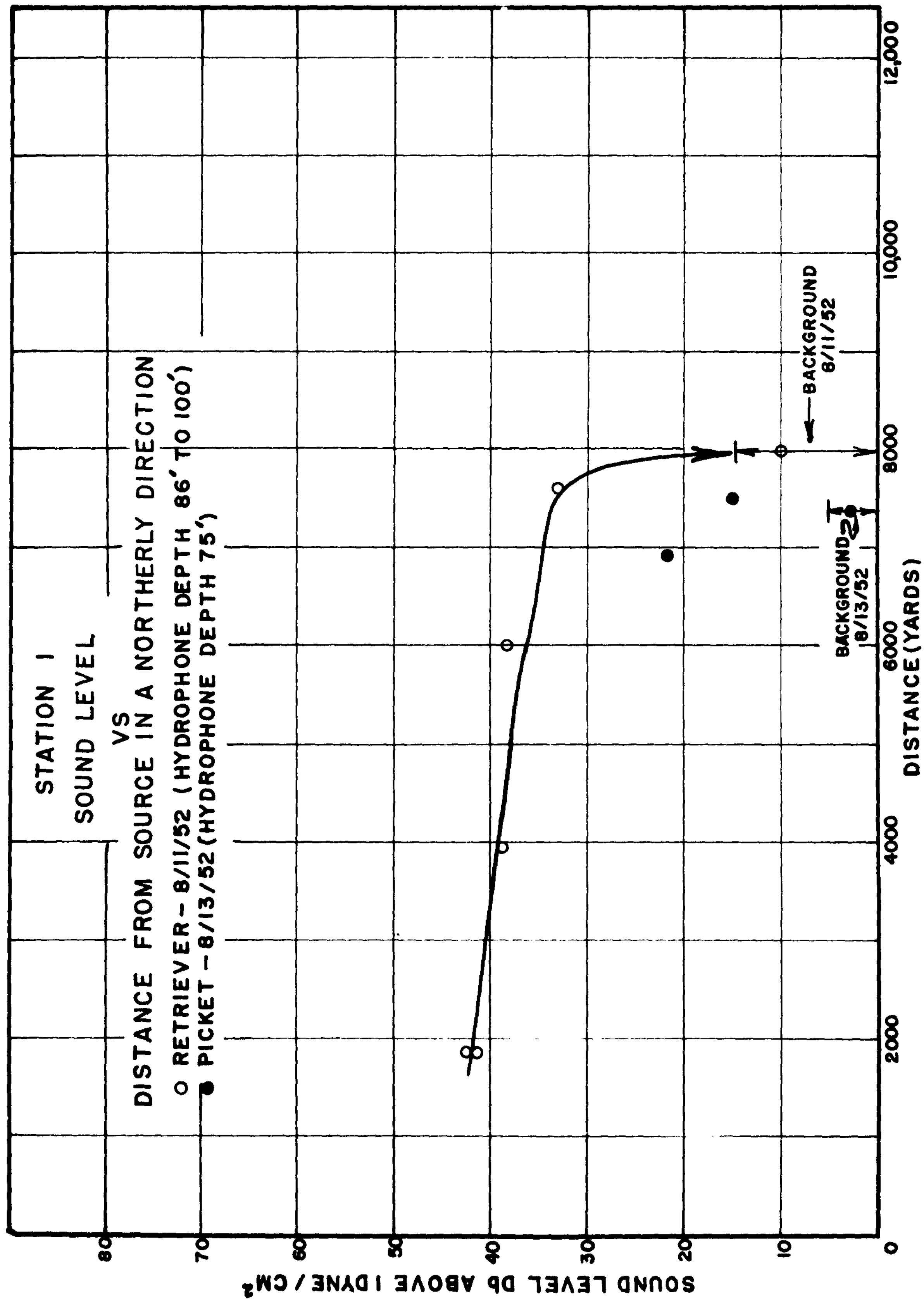

Figure 6

CONFIDENTIAL
SECURITY INFORMATION

CONFIDENTIAL
SECURITY INFORMATION

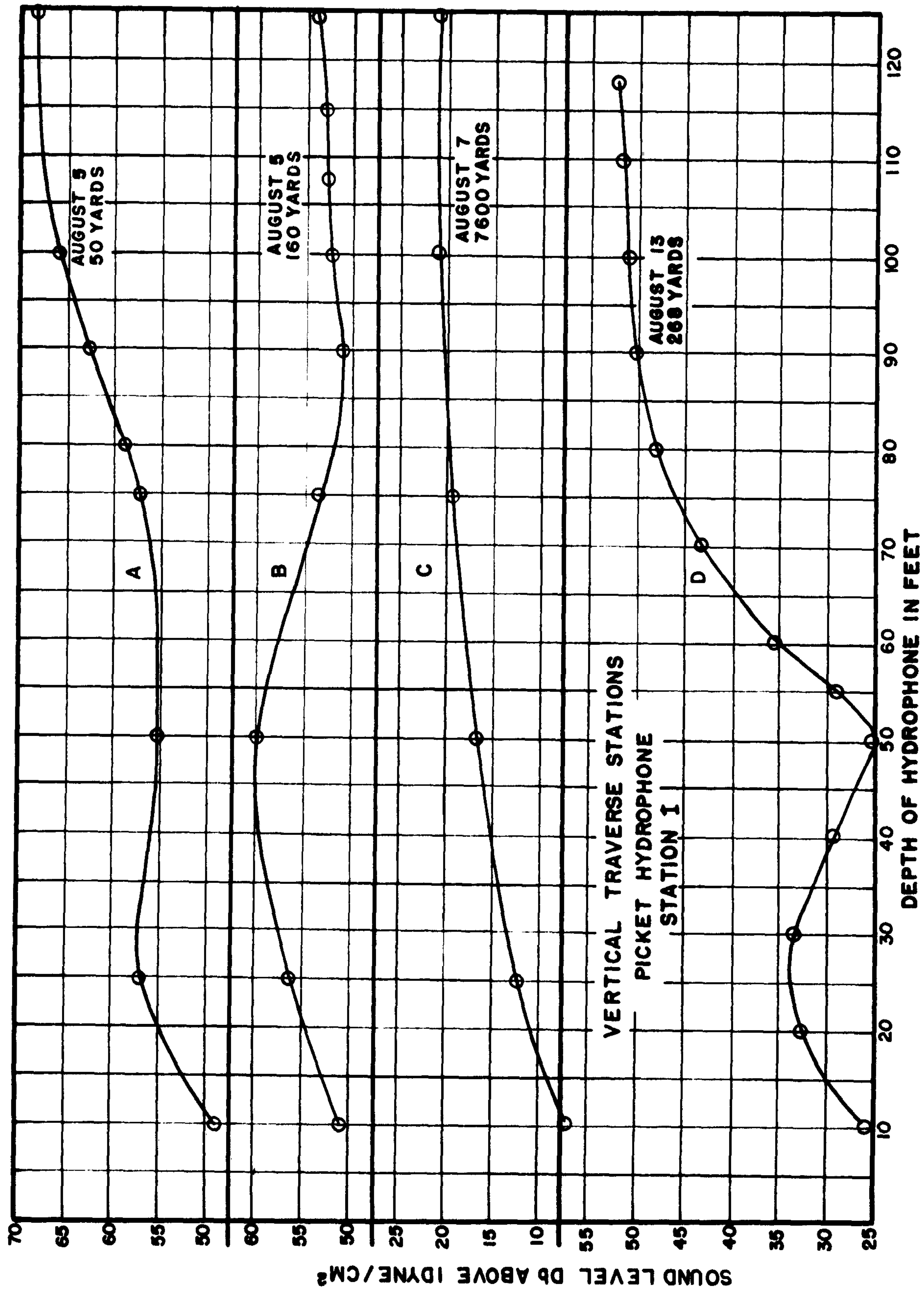

Figure 7

CONFIDENTIAL
SECURITY INFORMATION

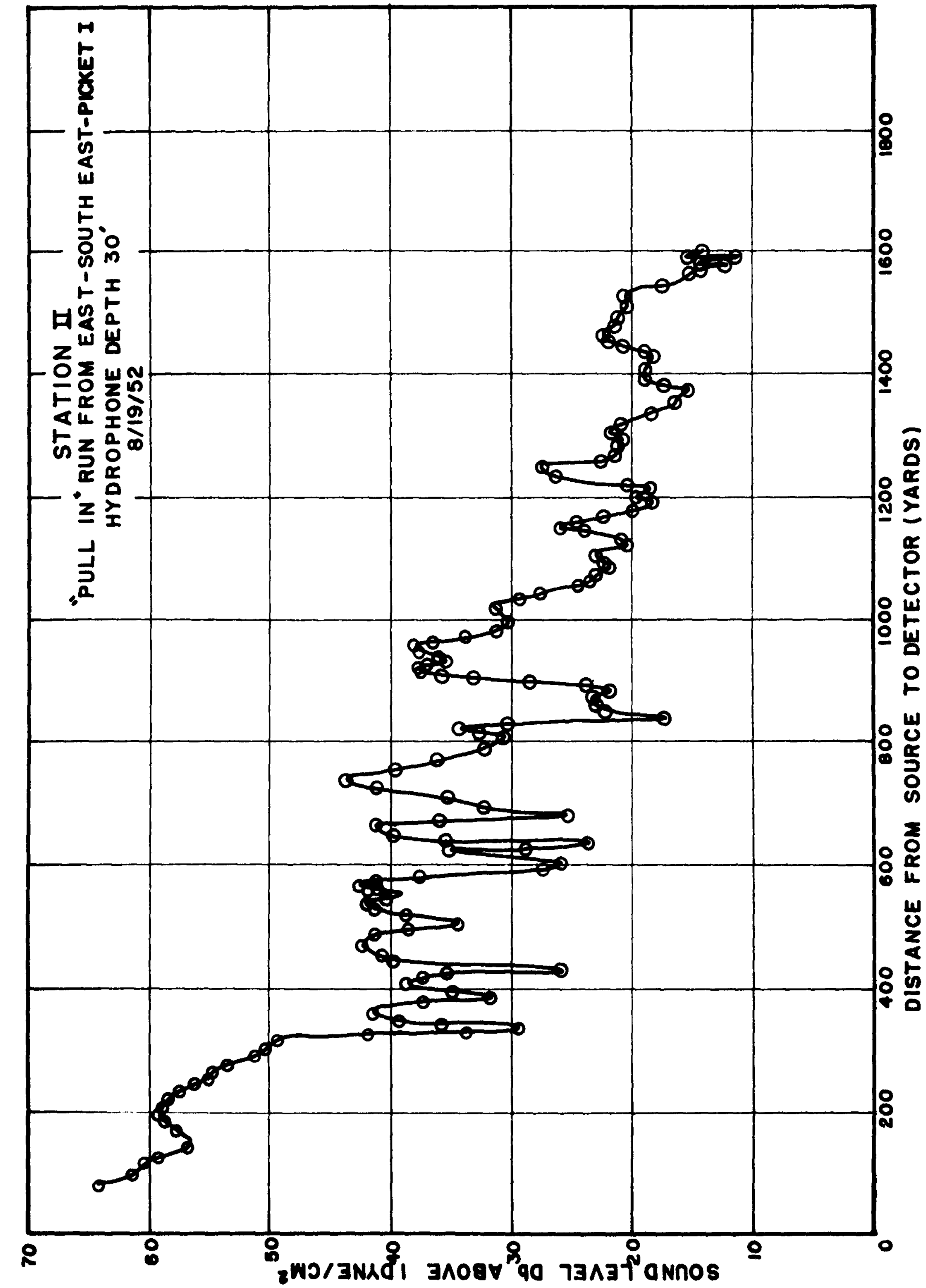
STATION II
"PULL IN" RUN FROM EAST-SOUTH EAST-PICKET I
HYDROPHONE DEPTH 30'
8/19/52
DISTANCE FROM SOURCE TO DETECTOR (YARDS)
0
200
400
600
800
1000
1200
1400
1600
1800
SOUND LEVEL Db ABOVE 1 DYNE/CM²
70
60
50
40
30
20
10
0

Figure 8

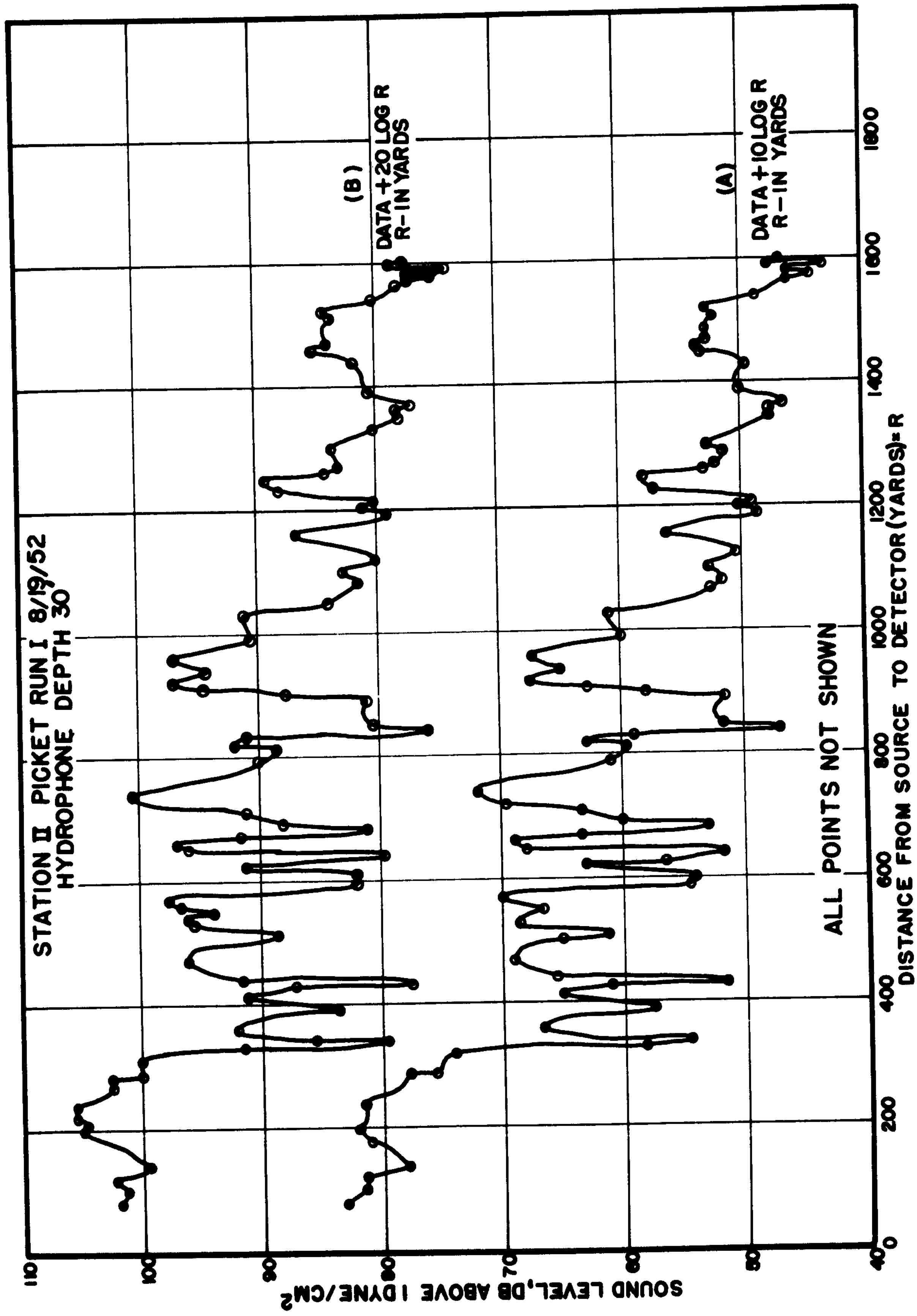
STATION II PICKET RUN I 8/19/52
HYDROPHONE DEPTH 30'
(B)
DATA +20 LOG R
R-IN YARDS
(A)
DATA +10 LOG R
R-IN YARDS
ALL POINTS NOT SHOWN
DISTANCE FROM SOURCE TO DETECTOR (YARDS) = R
SOUND LEVEL, DB ABOVE 1 DYNE/CM²
0
200
400
600
800
1000
1200
1400
1600
1800
40
50
60
70
80
90
100
110

Figure 8A & 8B

CONFIDENTIAL
SECURITY INFORMATION

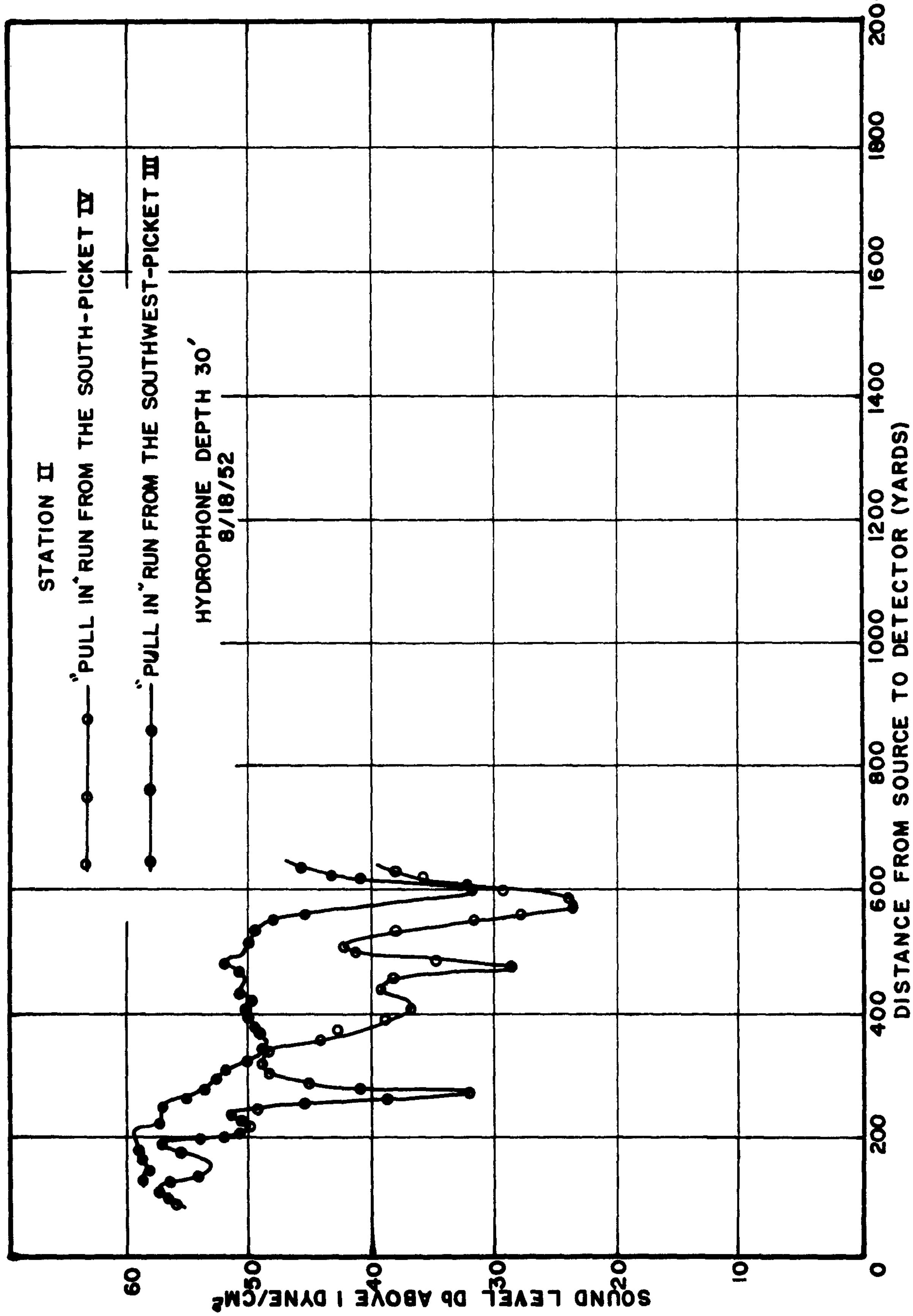

Figure 9

CONFIDENTIAL
SECURITY INFORMATION

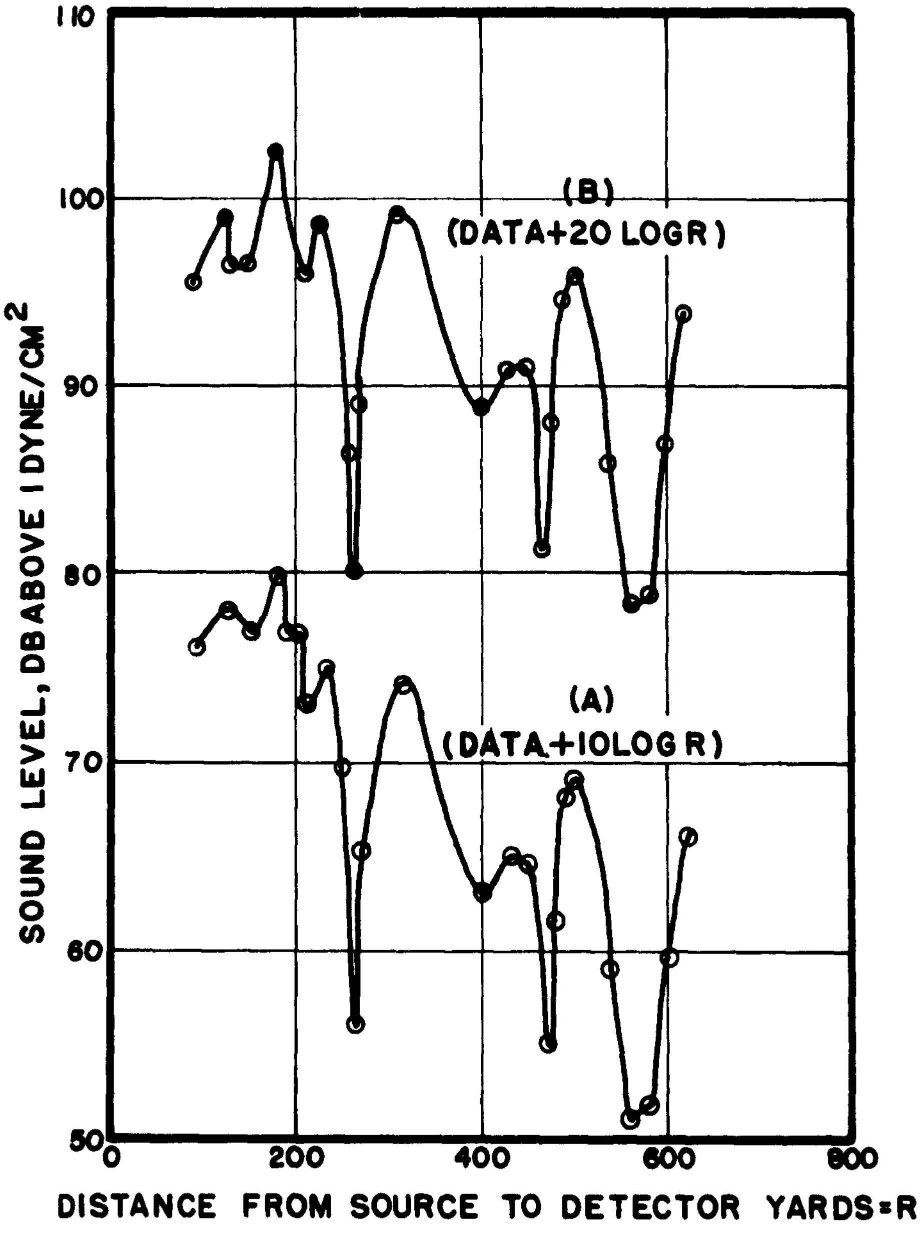

(ALL POINTS NOT SHOWN)

STATION II: PICKET IV RUNS 8/18/52
HYDROPHONE DEPTH 30'

Figure 9A & 9B

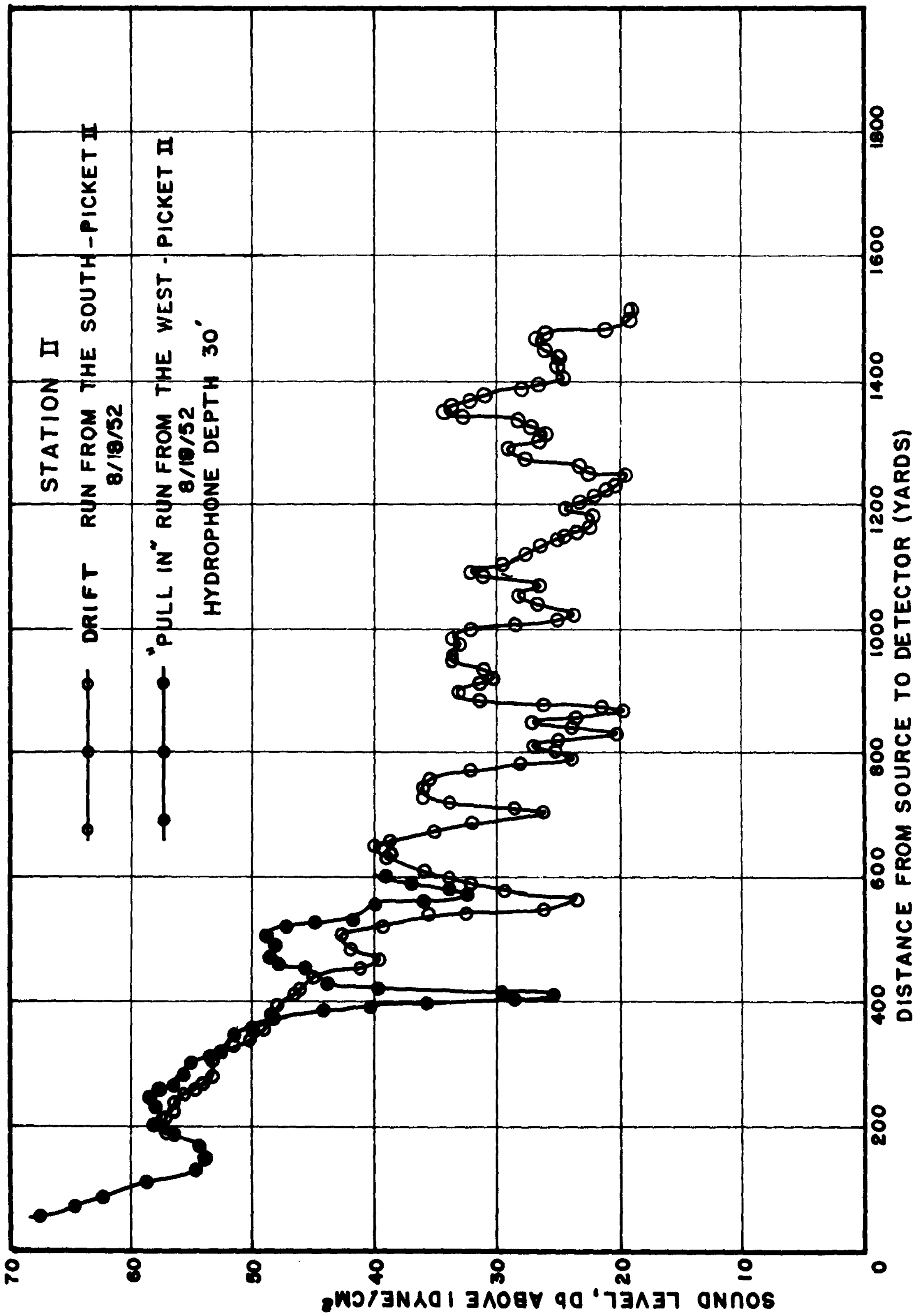
STATION II
DRIFT RUN FROM THE SOUTH - PICKET II
8/18/52
"PULL IN" RUN FROM THE WEST - PICKET II
8/18/52
HYDROPHONE DEPTH 30'
DISTANCE FROM SOURCE TO DETECTOR (YARDS)
SOUND LEVEL, DB ABOVE 1 DYNE/CM²
0
200
400
600
800
1000
1200
1400
1600
1800
0
10
20
30
40
50
60
70

Figure 10

CONFIDENTIAL
SECURITY INFORMATION

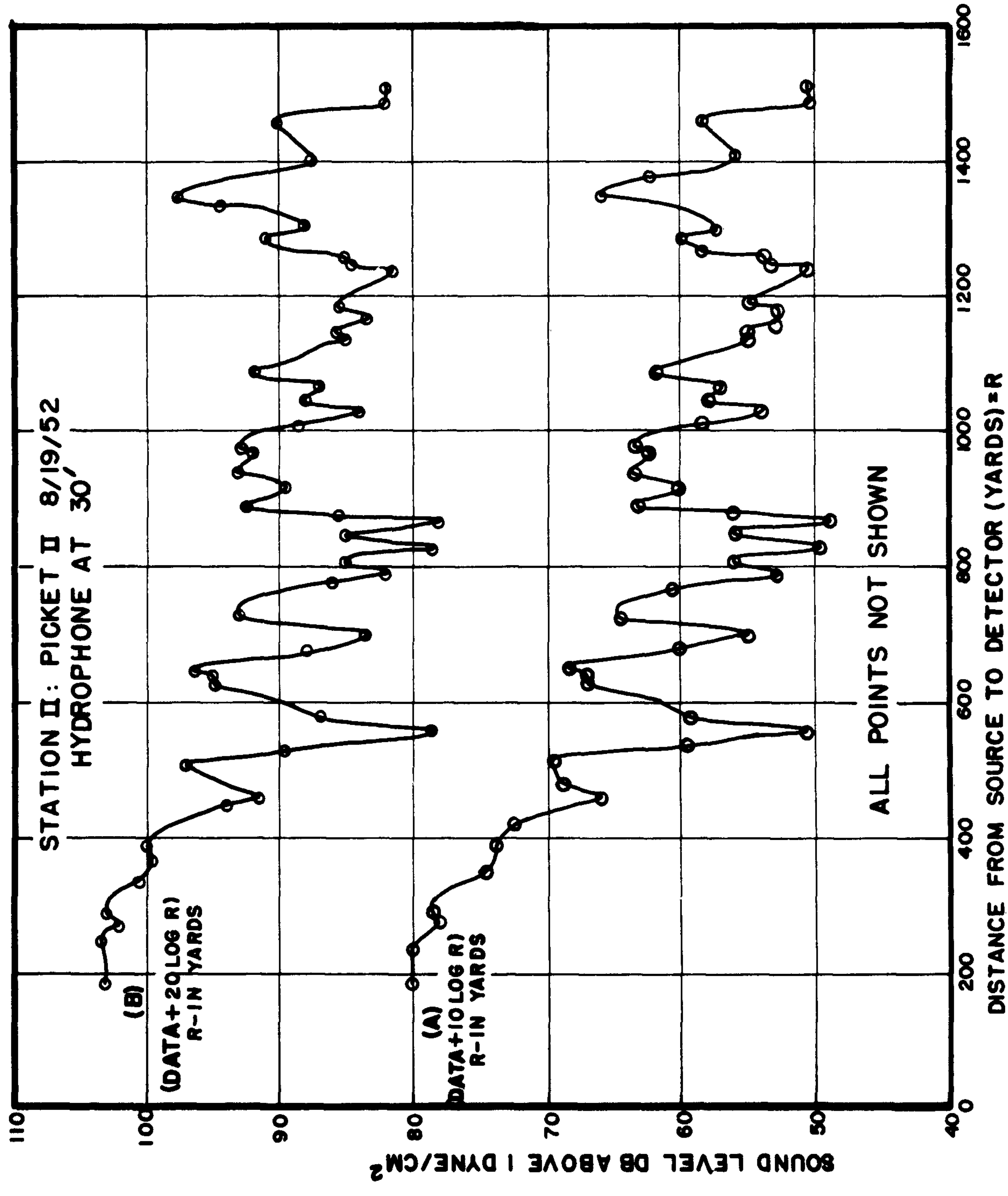

Figure 10A & 10B

CONFIDENTIAL
SECURITY INFORMATION

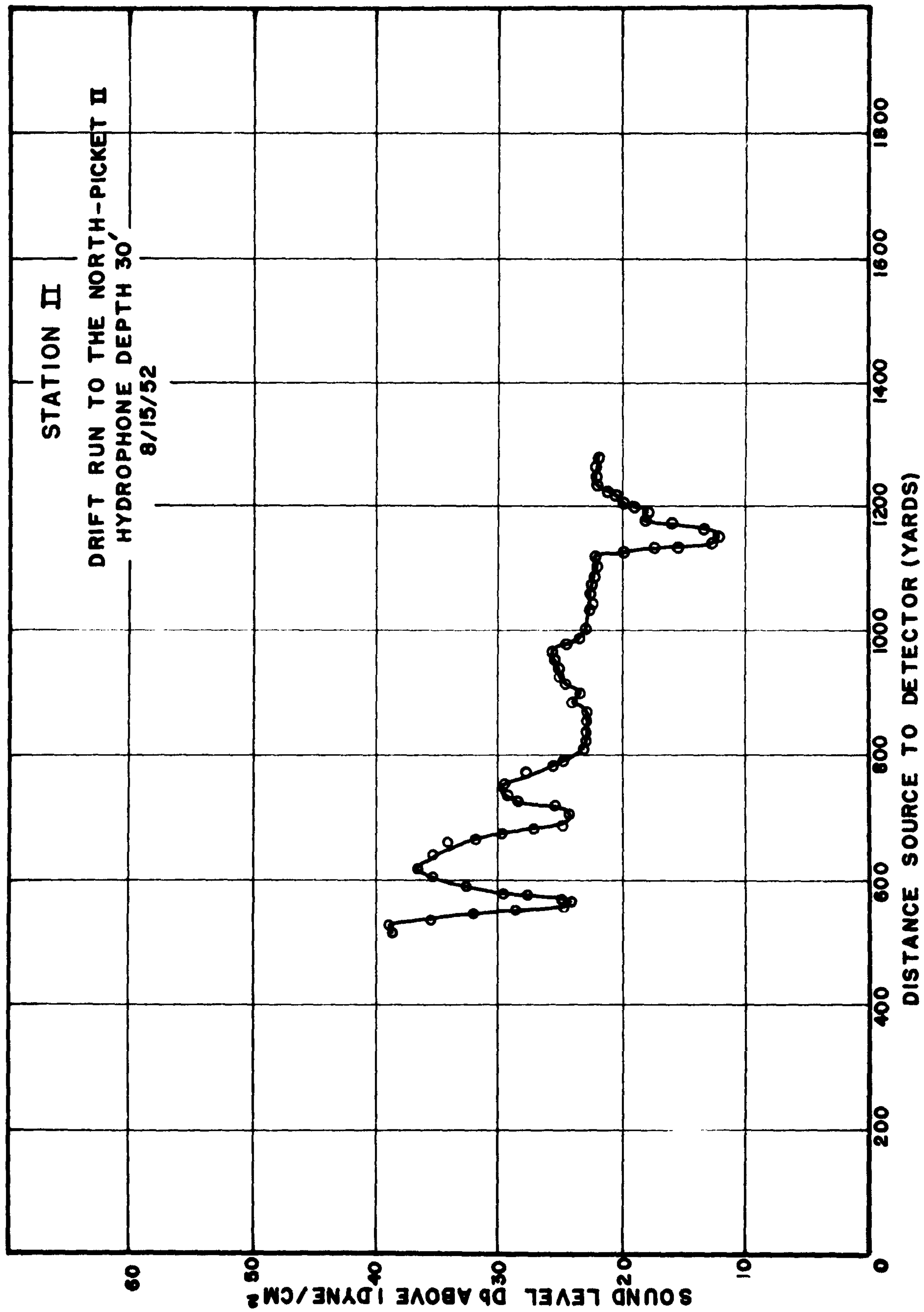
STATION II
DRIFT RUN TO THE NORTH-PICKET II
HYDROPHONE DEPTH 30'
8/15/52
DISTANCE SOURCE TO DETECTOR (YARDS)
0
200
400
600
800
1000
1200
1400
1600
1800
SOUND LEVEL DB ABOVE 1 DYNE/CM²
0
10
20
30
40
50
60

Figure 11

STATION II : PICKET RUN II 8/15/52
HYDROPHONE DEPTH 30'

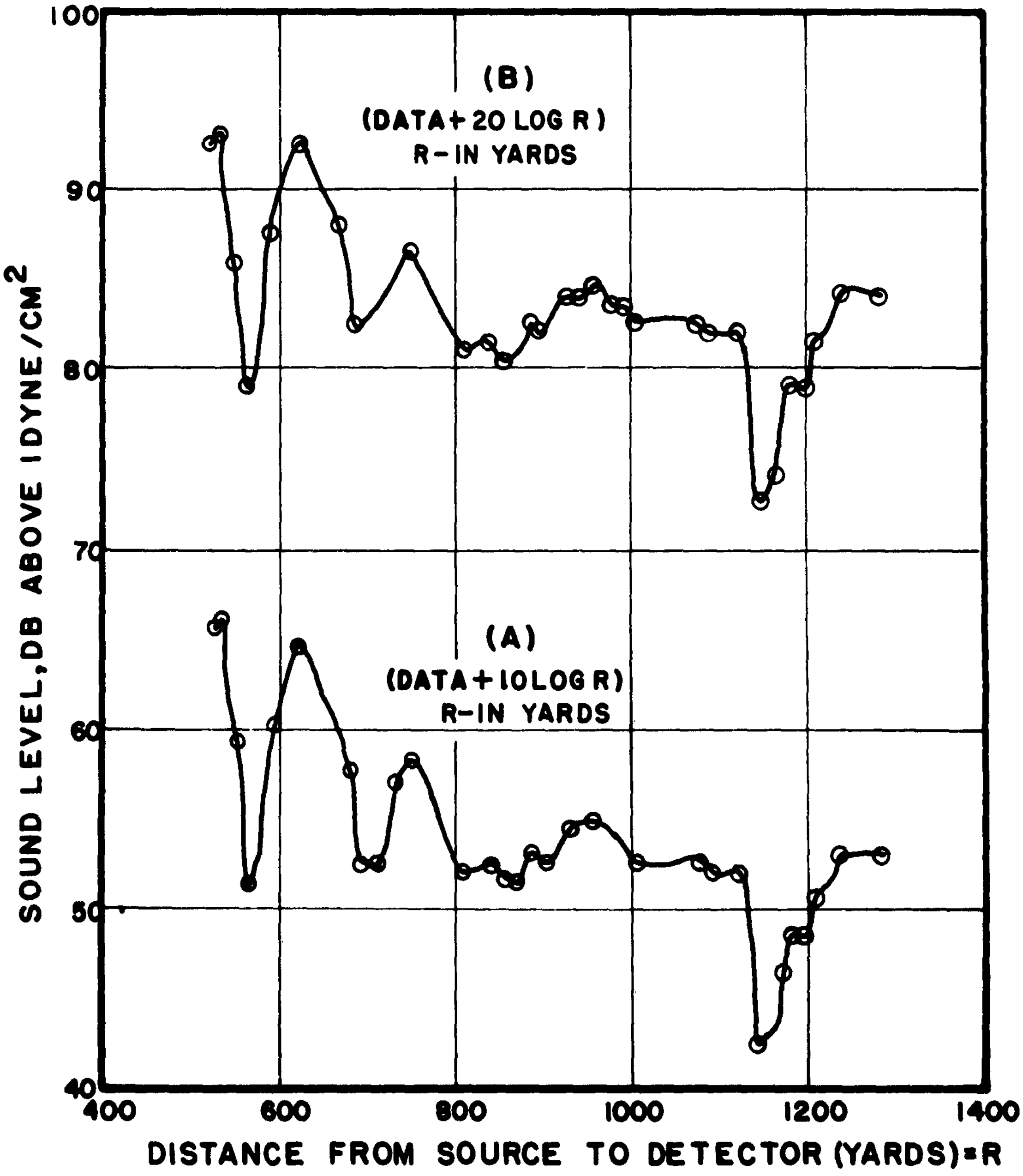

(ALL POINTS NOT SHOWN)

Figure 11A & 11B

STATION II
DRIFT RUN TO THE NORTH EAST-RETRIEVER I
HYDROPHONE DEPTH 25'
8/15/52

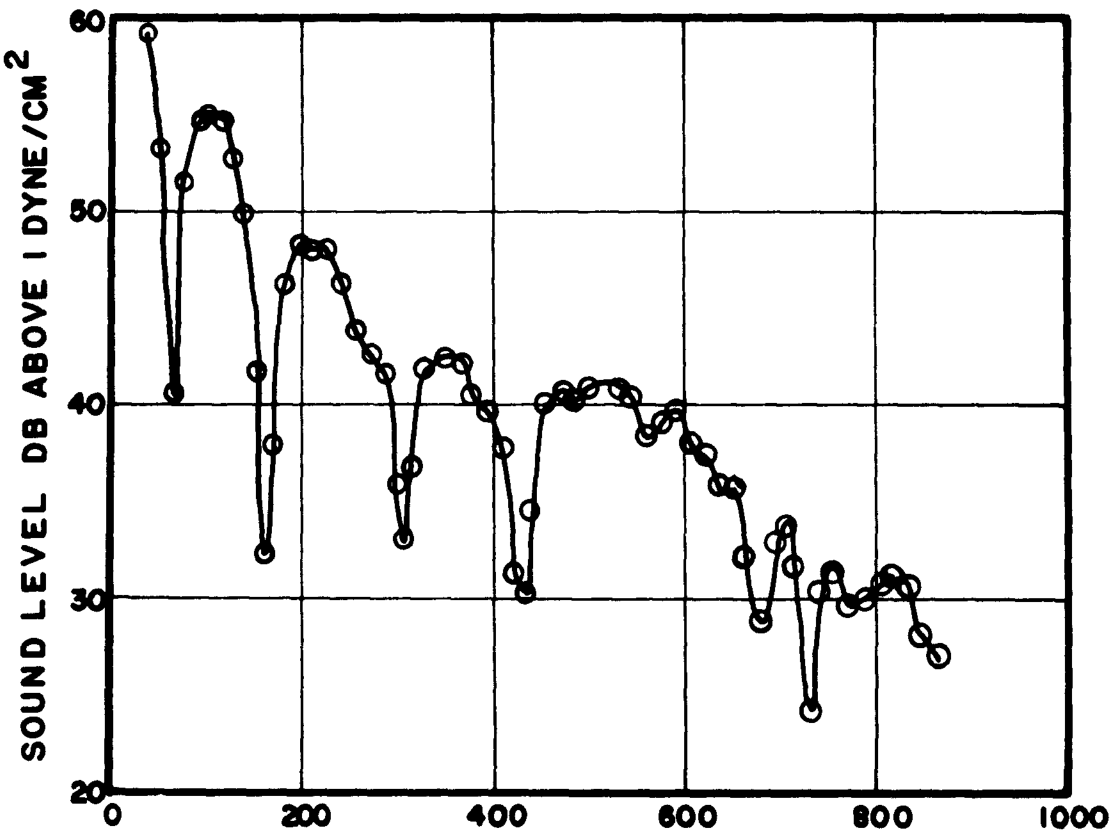

Figure 12

CONFIDENTIAL
SECURITY INFORMATION

STATION II

DRIFT RUN TO THE NORTH-EAST
HYDROPHONE DEPTH 25'- RETRIEVER I
8/15/52

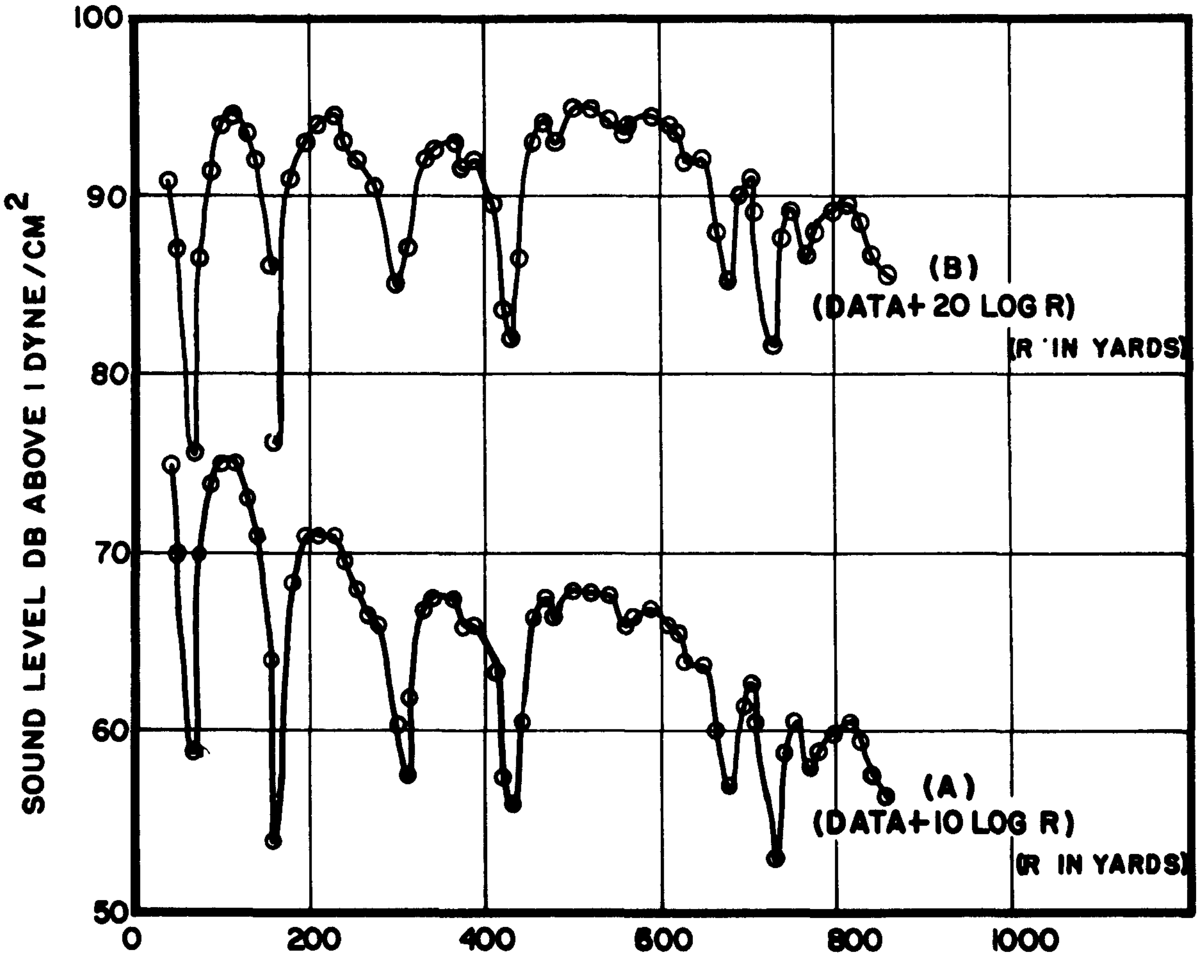

Figure 12A & 12B

CONFIDENTIAL
SECURITY INFORMATION

CONFIDENTIAL
SECURITY INFORMATION

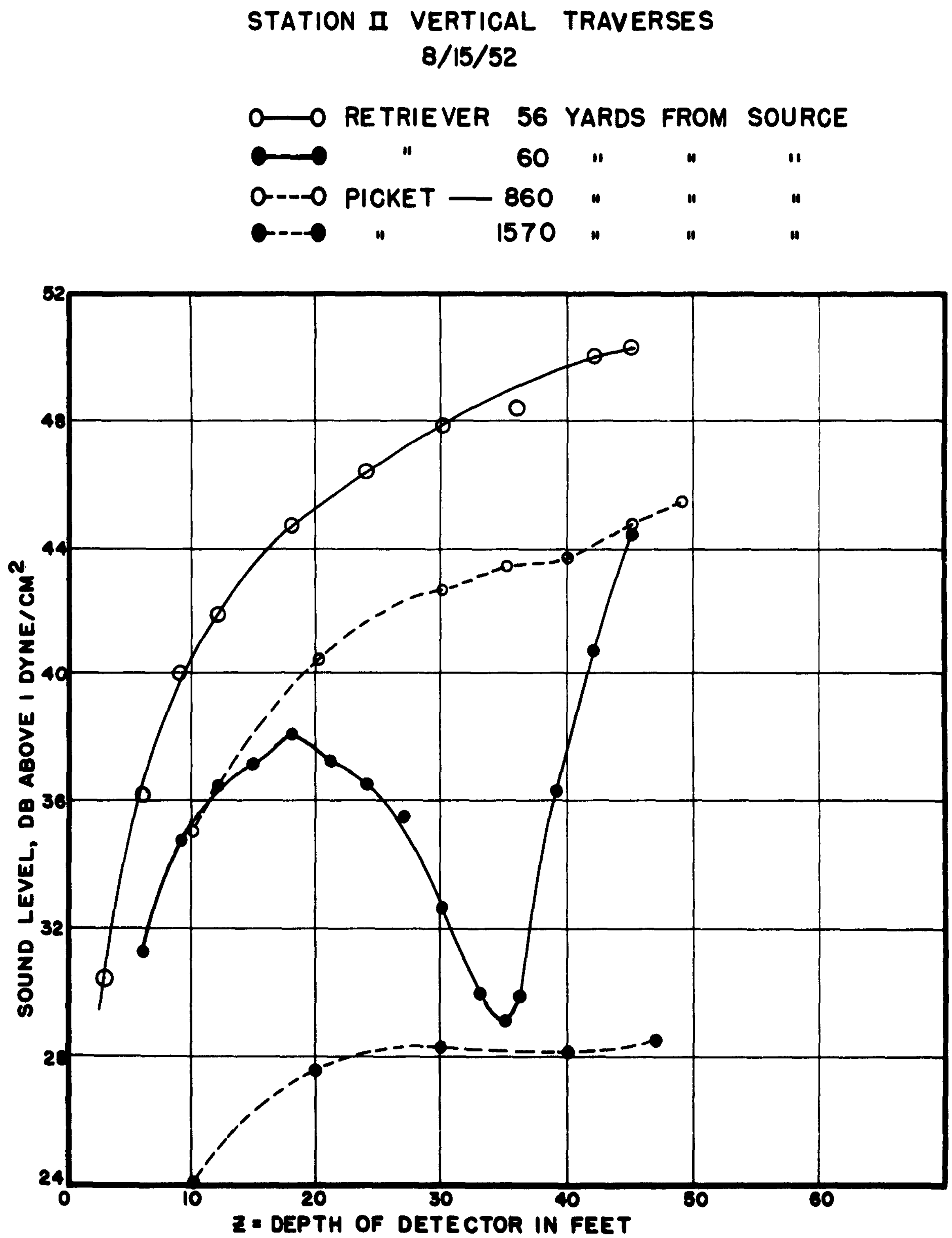

Figure 13

CONFIDENTIAL
SECURITY INFORMATION

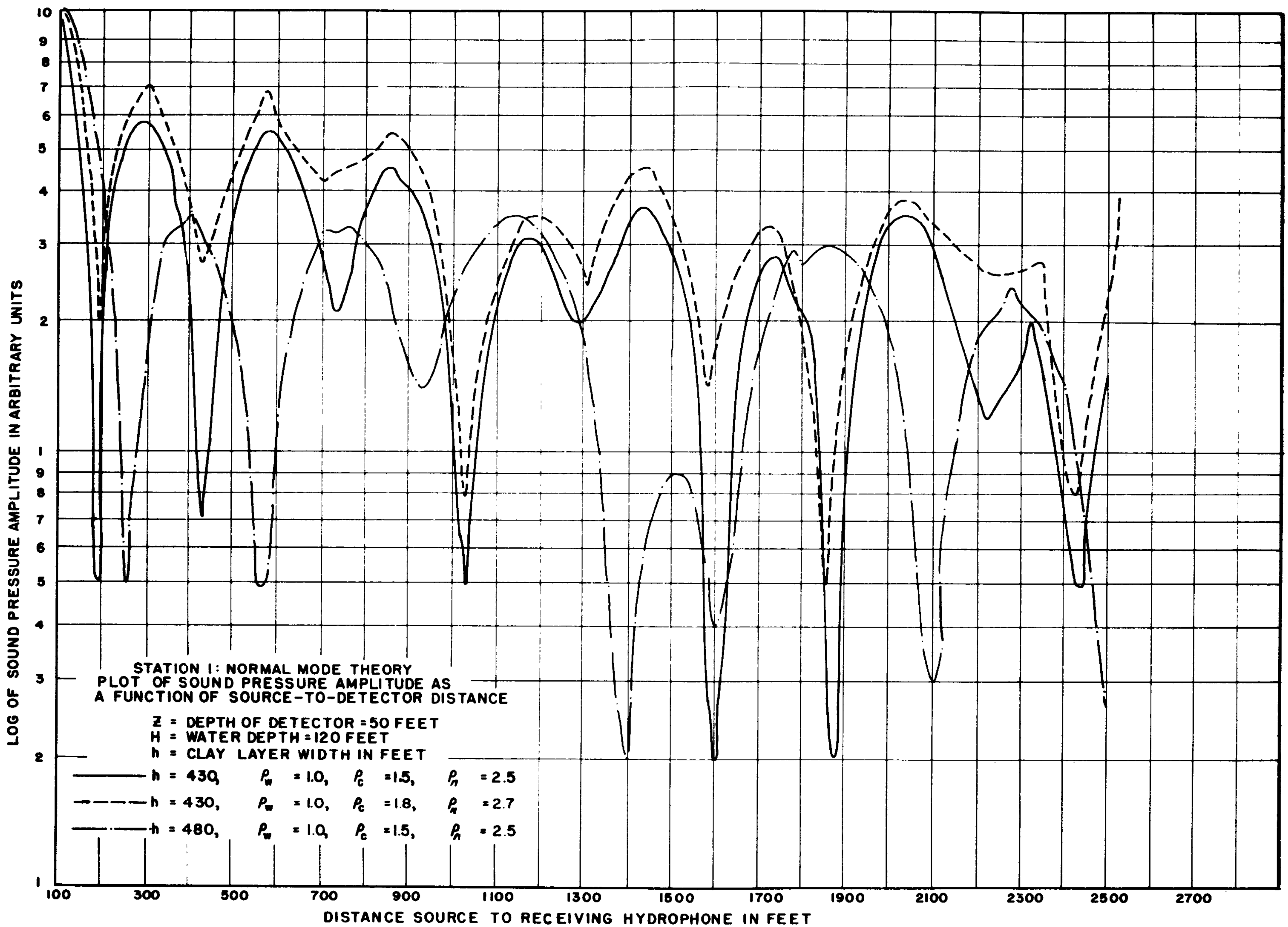
10
9
8
7
6
5
4
3
2
1
9
8
7
6
5
4
3
2
1
LOG OF SOUND PRESSURE AMPLITUDE IN ARBITRARY UNITS
100
300
500
700
900
1100
1300
1500
1700
1900
2100
2300
2500
2700
DISTANCE SOURCE TO RECEIVING HYDROPHONE IN FEET
STATION I: NORMAL MODE THEORY
PLOT OF SOUND PRESSURE AMPLITUDE AS
A FUNCTION OF SOURCE-TO-DETECTOR DISTANCE
Z = DEPTH OF DETECTOR = 50 FEET
H = WATER DEPTH = 120 FEET
h = CLAY LAYER WIDTH IN FEET
h = 430, ρw = 1.0, ρc = 1.5, ρn = 2.5
h = 430, ρw = 1.0, ρc = 1.8, ρn = 2.7
h = 480, ρw = 1.0, ρc = 1.5, ρn = 2.5

Figure 14

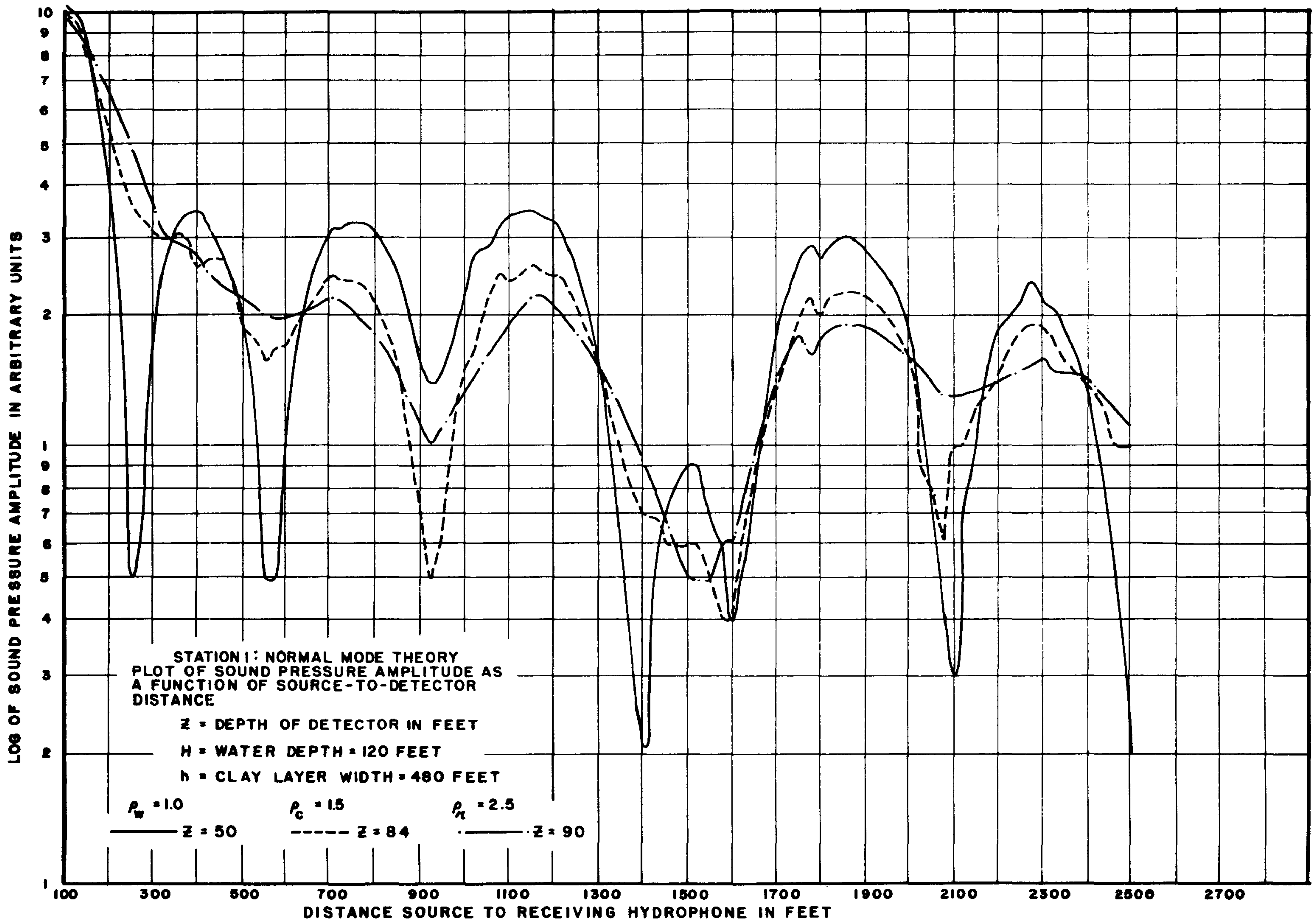
10
9
8
7
6
5
4
3
2
1
9
8
7
6
5
4
3
2
1
LOG OF SOUND PRESSURE AMPLITUDE IN ARBITRARY UNITS
100
300
500
700
900
1100
1300
1500
1700
1900
2100
2300
2500
2700
DISTANCE SOURCE TO RECEIVING HYDROPHONE IN FEET
STATION I: NORMAL MODE THEORY
PLOT OF SOUND PRESSURE AMPLITUDE AS A FUNCTION OF SOURCE-TO-DETECTOR DISTANCE
Z = DEPTH OF DETECTOR IN FEET
H = WATER DEPTH = 120 FEET
h = CLAY LAYER WIDTH = 480 FEET
ρ_w = 1.0
ρ_c = 1.5
ρ_r = 2.5
Z = 50
Z = 84
Z = 90

Figure 15

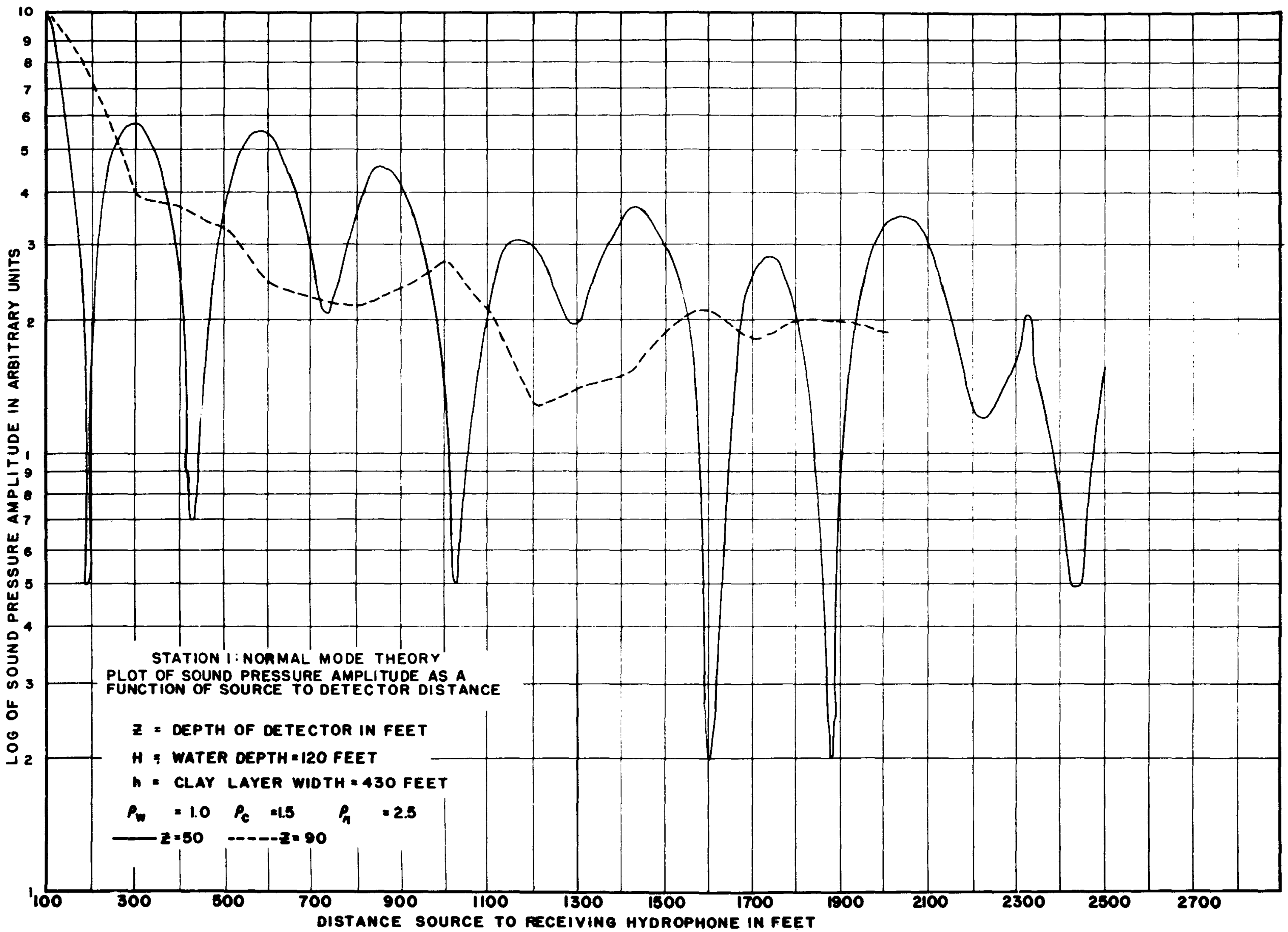
10
9
8
7
6
5
4
3
2
1
9
8
7
6
5
4
3
2
1
LOG OF SOUND PRESSURE AMPLITUDE IN ARBITRARY UNITS
100
300
500
700
900
1100
1300
1500
1700
1900
2100
2300
2500
2700
DISTANCE SOURCE TO RECEIVING HYDROPHONE IN FEET
STATION I: NORMAL MODE THEORY
PLOT OF SOUND PRESSURE AMPLITUDE AS A FUNCTION OF SOURCE TO DETECTOR DISTANCE
Z = DEPTH OF DETECTOR IN FEET
H = WATER DEPTH = 120 FEET
h = CLAY LAYER WIDTH = 430 FEET
ρw = 1.0 ρc = 1.5 ρR = 2.5
—— Z = 50 ----- Z = 90

Figure 16

STATION I: NORMAL MODE THEORY PLOT OF SOUND PRESSURE AMPLITUDE AS A FUNCTION OF DETECTOR DEPTH FOR VARIOUS SOURCE-TO-DETECTOR DISTANCES

H = WATER DEPTH = 120 FEET

h = CLAY LAYER WIDTH = 480 FEET

$\rho_w = 1.0$ $\rho_c = 1.5$ $\rho_\eta = 2.5$

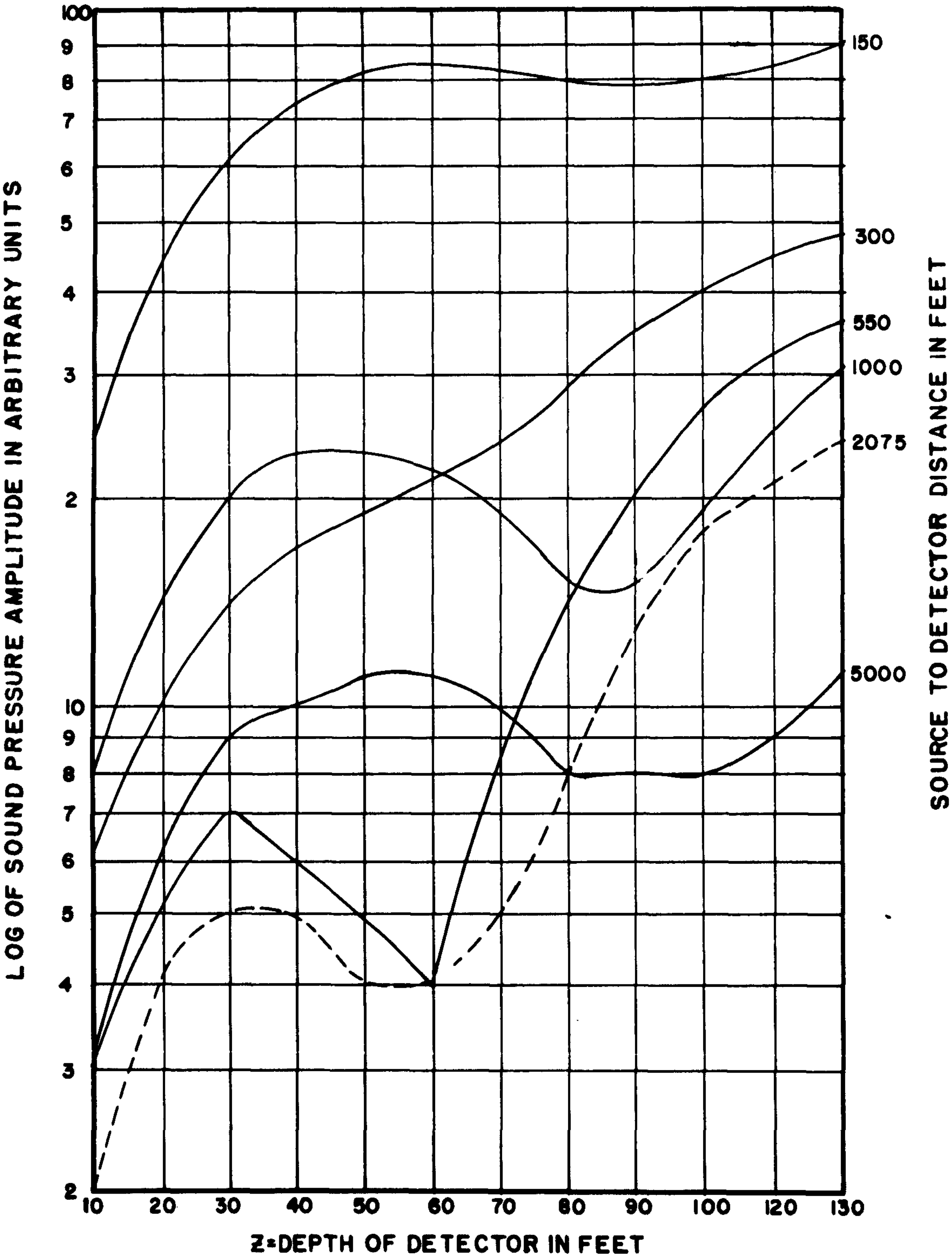

Figure 17

STATION I: NORMAL MODE THEORY PLOT OF SOUND PRESSURE AMPLITUDE AS A FUNCTION OF DETECTOR DEPTH FOR VARIOUS SOURCE-TO-DETECTOR DISTANCES

H = WATER DEPTH = 120 FEET

h = CLAY LAYER WIDTH = 480 FEET

$\rho_w = 1.0$ $\rho_c = 1.5$ $\rho_M = 2.5$

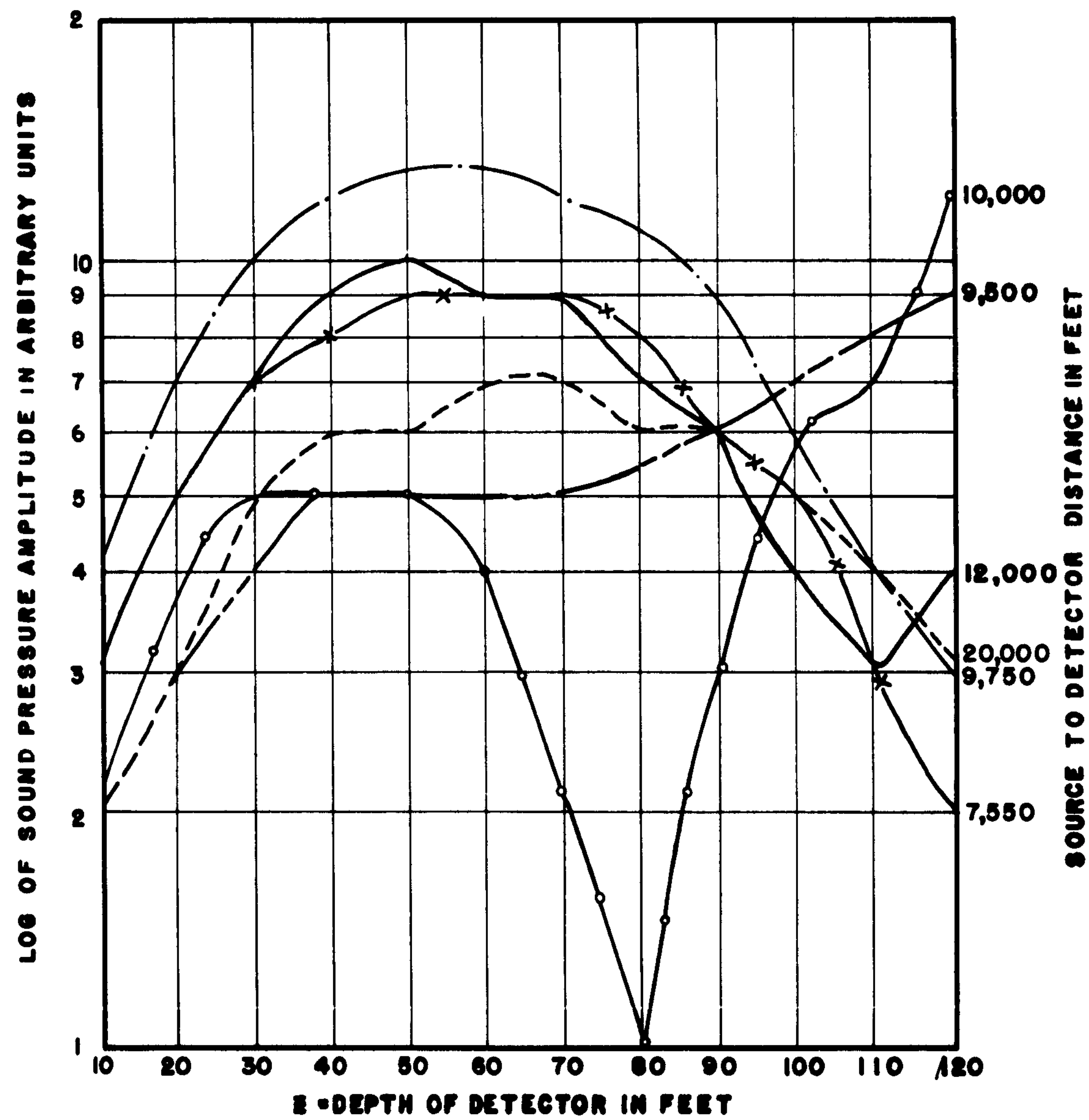

Figure 18

STATION II: NORMAL MODE THEORY
PLOT OF SOUND PRESSURE AMPLITUDE
AS A FUNCTION OF SOURCE-TO-DETECTOR-
DISTANCE

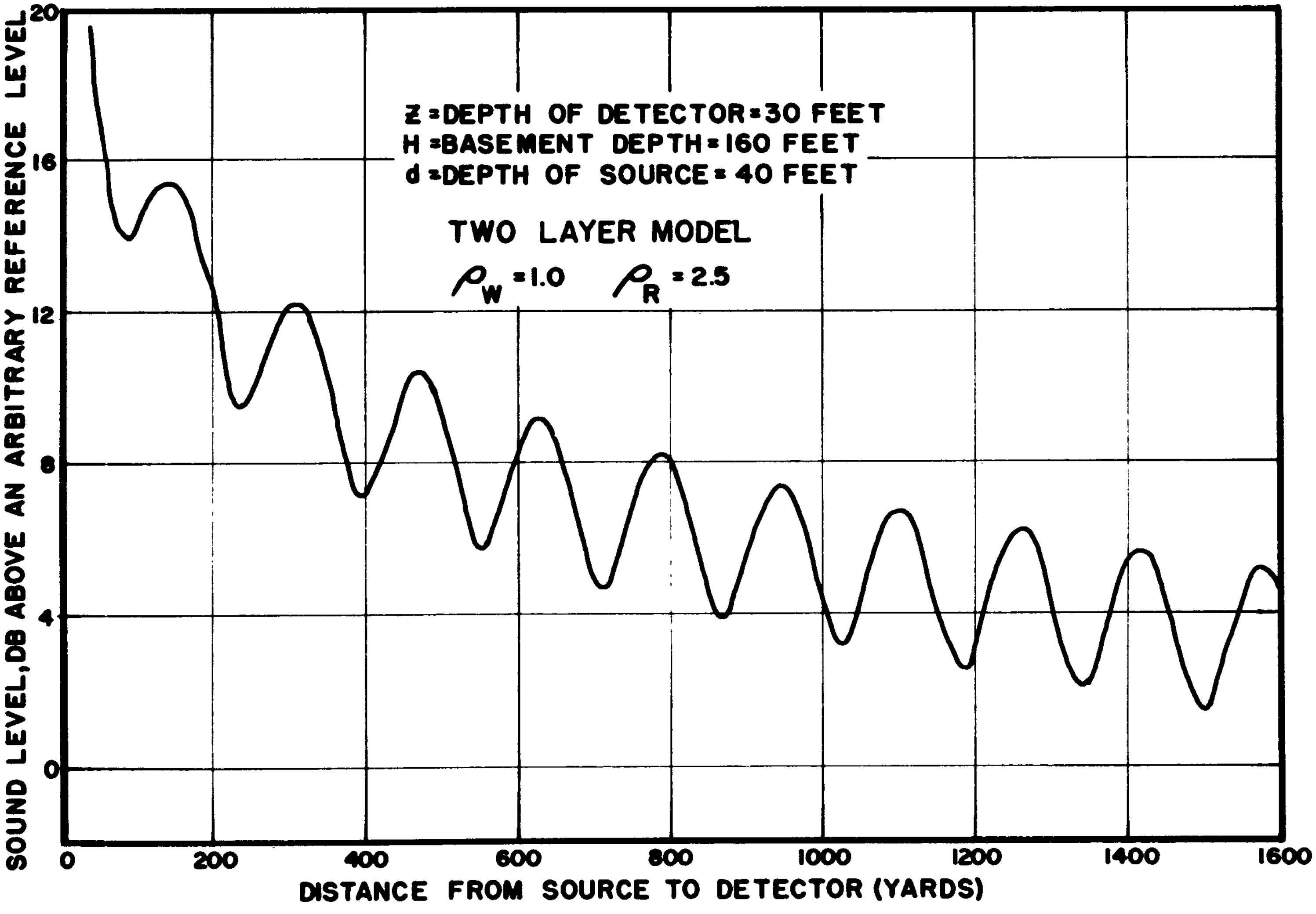

Figure 19

STATION II: NORMAL MODE THEORY
PLOT OF SOUND PRESSURE AMPLITUDE
AS A FUNCTION OF DETECTOR DEPTH

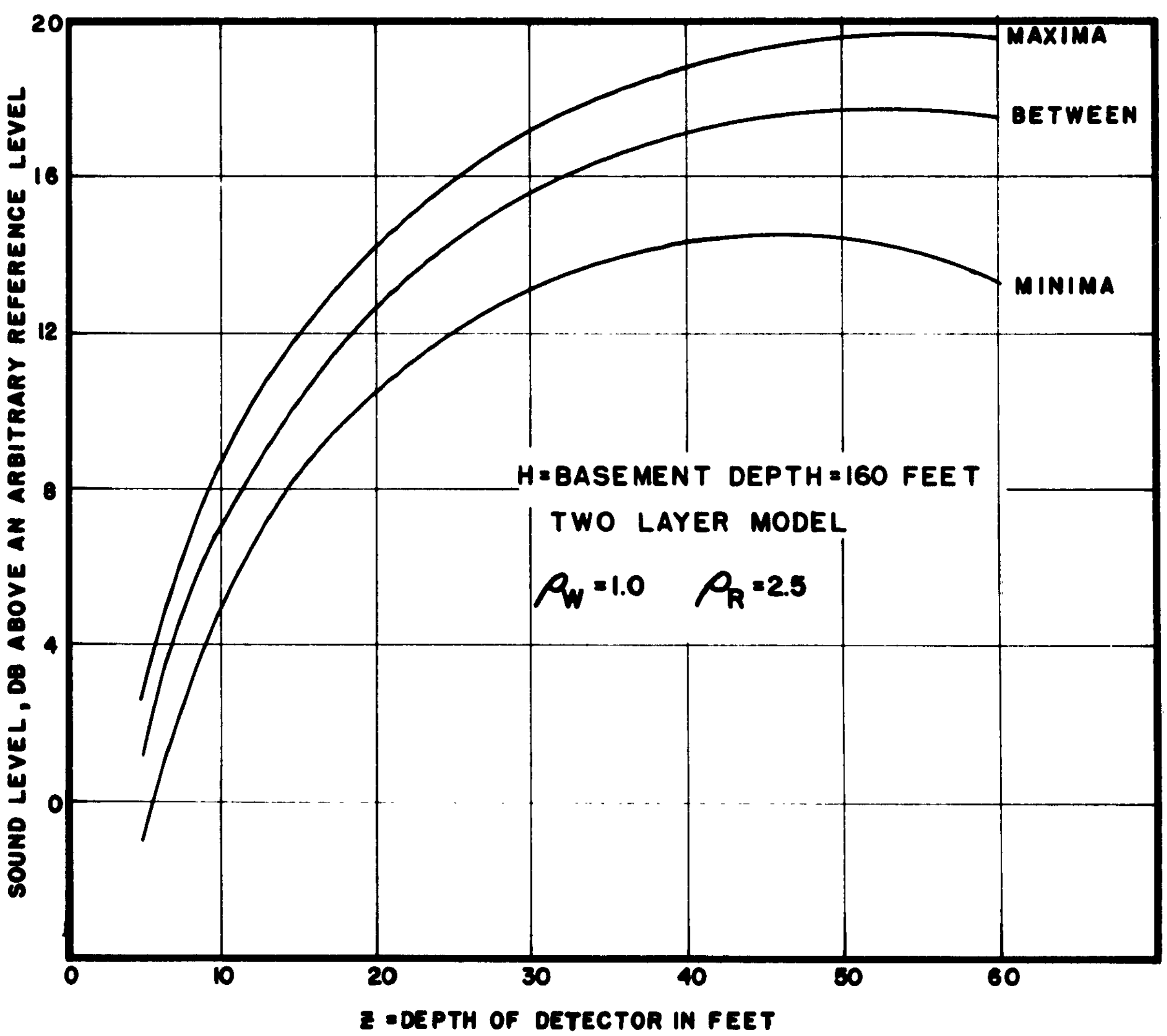

Figure 20

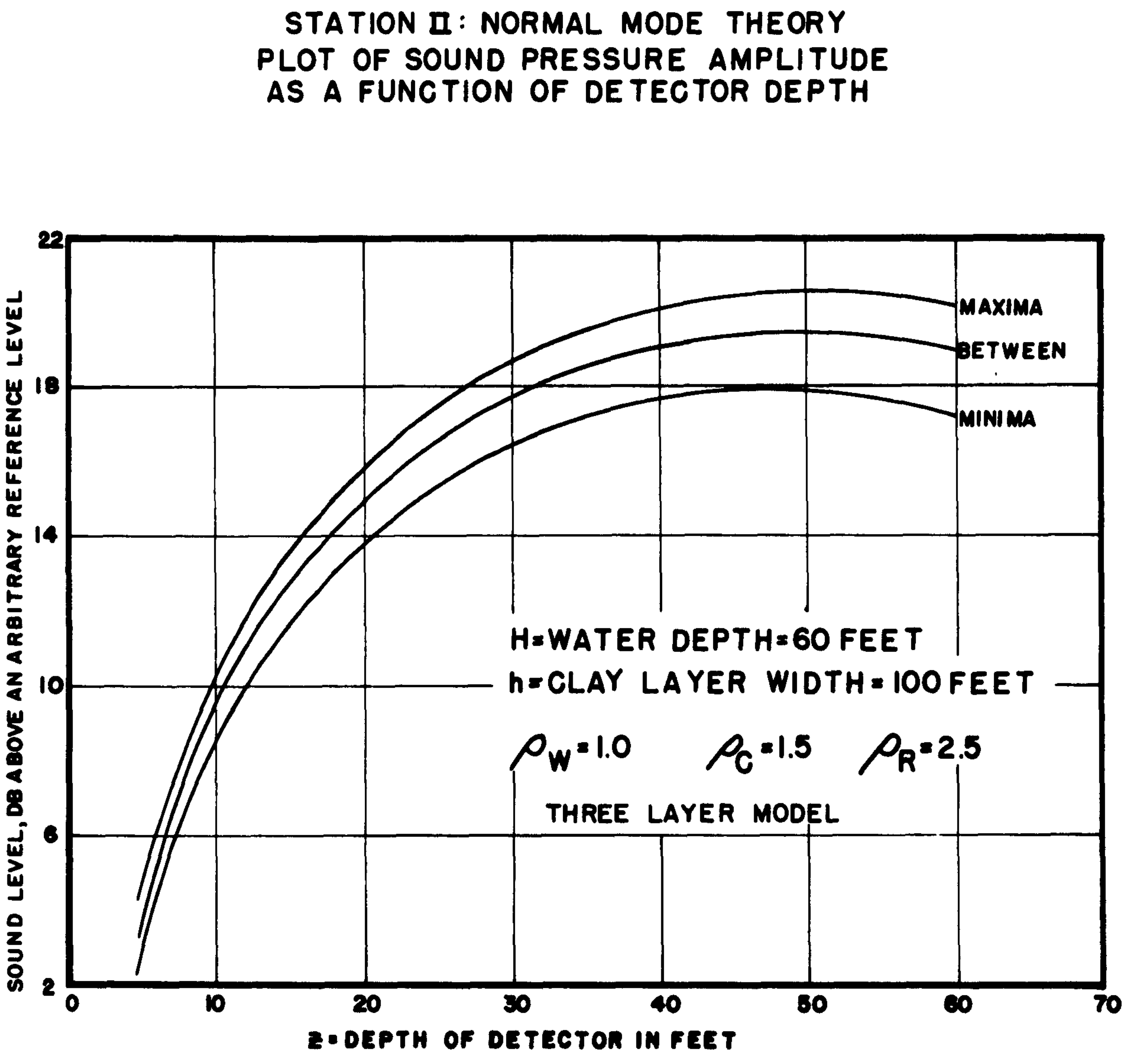
STATION II: NORMAL MODE THEORY
PLOT OF SOUND PRESSURE AMPLITUDE
AS A FUNCTION OF DETECTOR DEPTH
SOUND LEVEL, DB ABOVE AN ARBITRARY REFERENCE LEVEL
22
18
14
10
6
2
0
10
20
30
40
50
60
70
z = DEPTH OF DETECTOR IN FEET
MAXIMA
BETWEEN
MINIMA
H = WATER DEPTH = 60 FEET
h = CLAY LAYER WIDTH = 100 FEET
ρW = 1.0
ρC = 1.5
ρR = 2.5
THREE LAYER MODEL

Figure 21

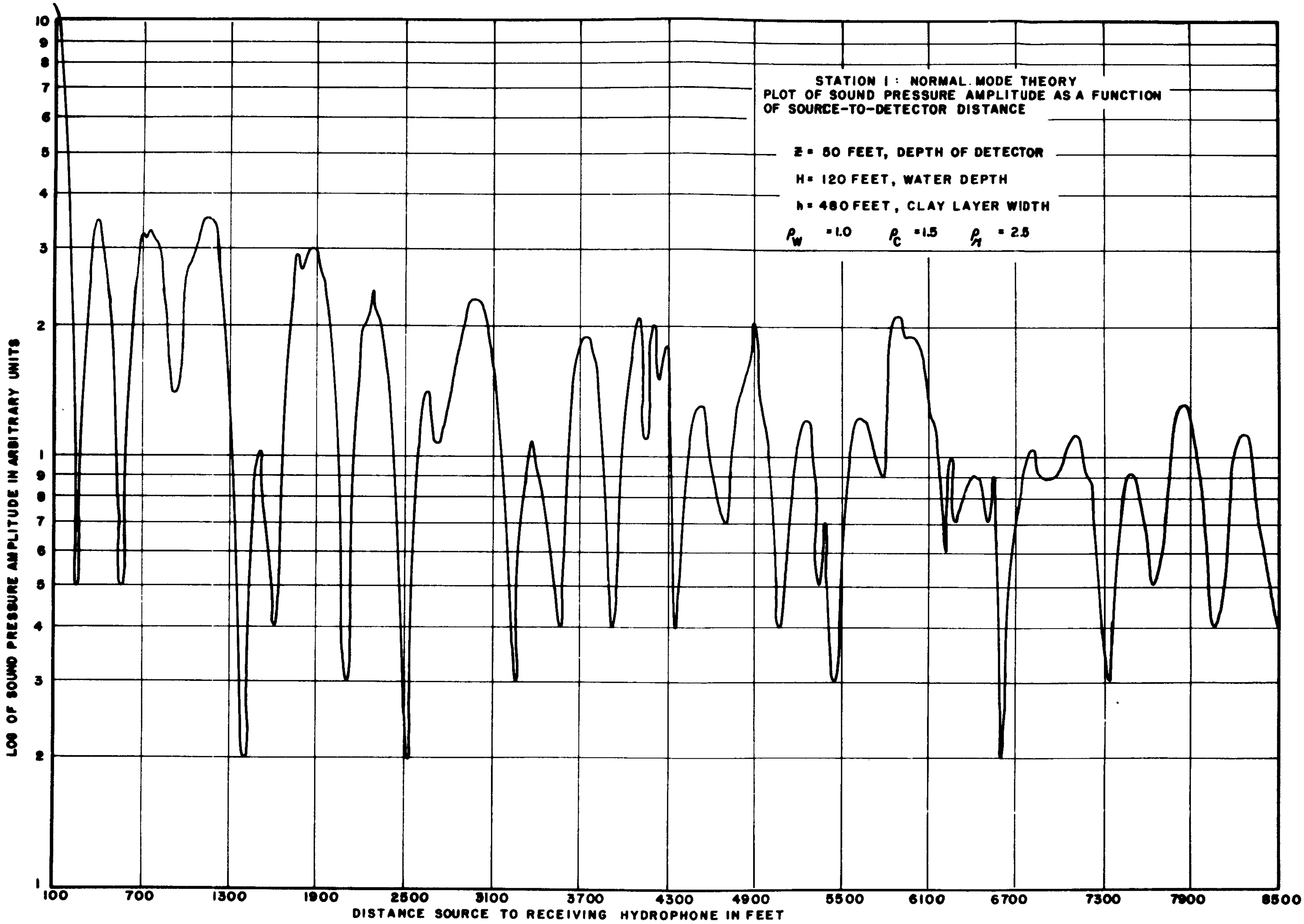
STATION I : NORMAL MODE THEORY
PLOT OF SOUND PRESSURE AMPLITUDE AS A FUNCTION OF SOURCE-TO-DETECTOR DISTANCE
z = 50 FEET, DEPTH OF DETECTOR
H = 120 FEET, WATER DEPTH
h = 480 FEET, CLAY LAYER WIDTH
ρ_W = 1.0 ρ_C = 1.5 ρ_1 = 2.5
LOG OF SOUND PRESSURE AMPLITUDE IN ARBITRARY UNITS
10
9
8
7
6
5
4
3
2
1
9
8
7
6
5
4
3
2
1
100
700
1300
1900
2500
3100
3700
4300
4900
5500
6100
6700
7300
7900
8500
DISTANCE SOURCE TO RECEIVING HYDROPHONE IN FEET

Figure 22

CONFIDENTIAL
SECURITY INFORMATION

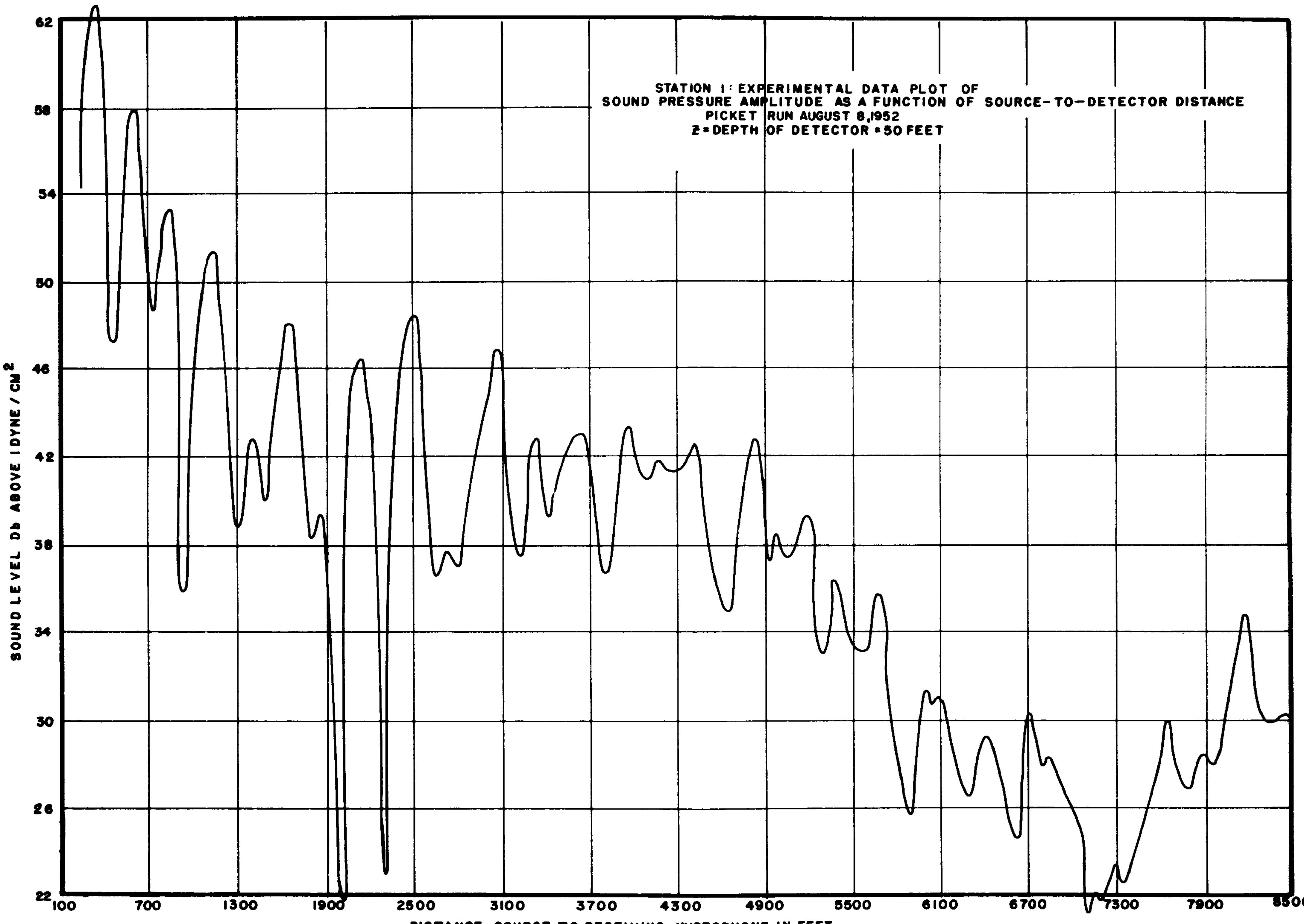

Figure 23

CONFIDENTIAL
SECURITY INFORMATION